



# High Resolution Elemental Mapping of Lunar Surface

Team 24 | ISRO High Prep Problem Statement

# OUTLINE

---



## 1 Introduction

X-ray Fluorescence  
Methodology

## 2 XRF Detection

Algorithm  
L Transition Lines  
Results

## 3 Mapping

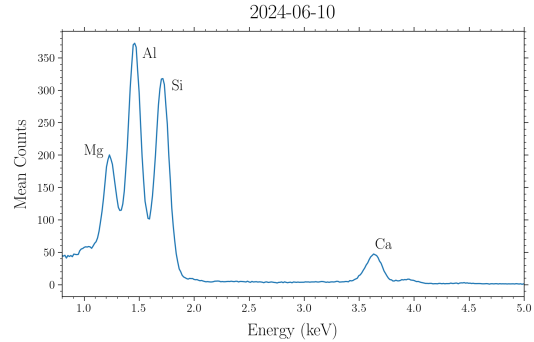
Methodology  
Results

## 4 Clustering

Ratio Selection  
1-D clustering  
2-D clustering

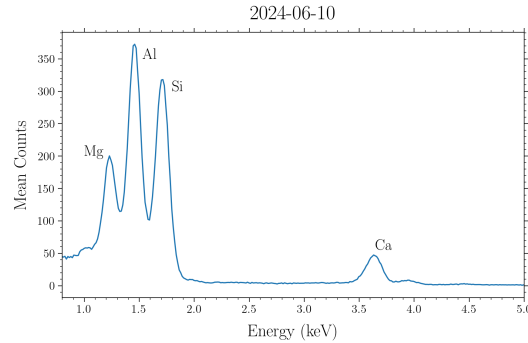
# X-RAY FLUORESCENCE

- » Emission of characteristic X-ray lines
- » Caused by high-energy external excitation, such as:
  - Solar radiation during solar flares
  - High energy synthetic beams
- » Non-destructive technique to find chemical composition



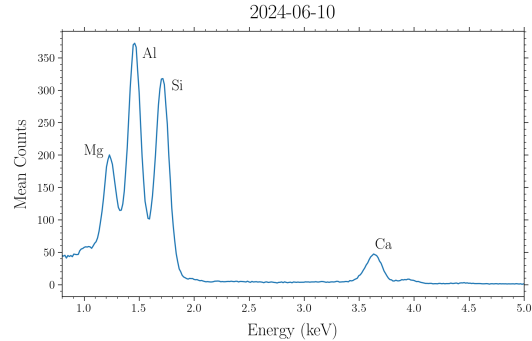
# X-RAY FLUORESCENCE

- » Emission of characteristic X-ray lines
- » Caused by high-energy external excitation, such as:
  - Solar radiation during solar flares
  - High energy synthetic beams
- » Non-destructive technique to find chemical composition



# X-RAY FLUORESCENCE

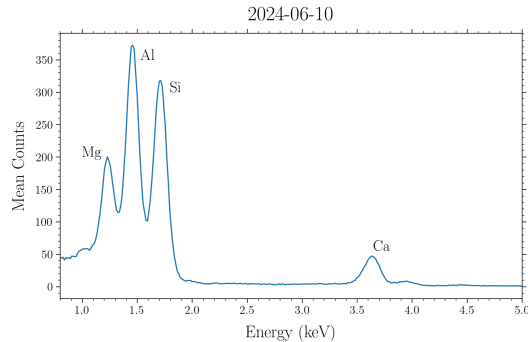
- » Emission of characteristic X-ray lines
- » Caused by high-energy external excitation, such as:
  - Solar radiation during solar flares
  - High energy synthetic beams
- » Non-destructive technique to find chemical composition



# X-RAY FLUORESCENCE



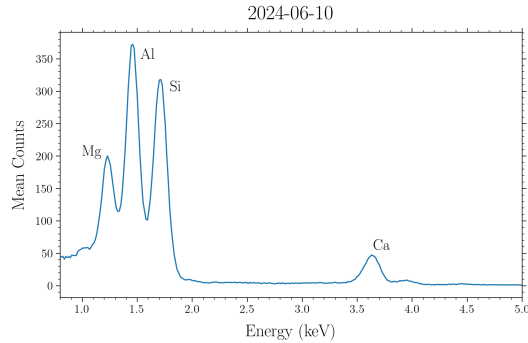
- » Emission of characteristic X-ray lines
- » Caused by high-energy external excitation, such as:
  - Solar radiation during solar flares
  - High energy synthetic beams
- » Non-destructive technique to find chemical composition



# X-RAY FLUORESCENCE



- » Emission of characteristic X-ray lines
- » Caused by high-energy external excitation, such as:
  - Solar radiation during solar flares
  - High energy synthetic beams
- » Non-destructive technique to find chemical composition



# METHODOLOGY

- » XRF detection using only CLASS data
  - Background model
  - Detection of elemental lines
- » Ratio between lines & uncertainties
  - Solar spectrum isn't needed, thus increasing overall data available
- » Mapping onto a lunar base map
- » Clustering, best ratios and compositional groups

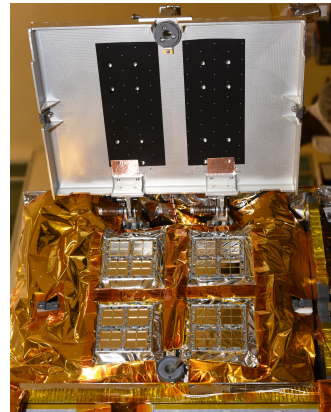
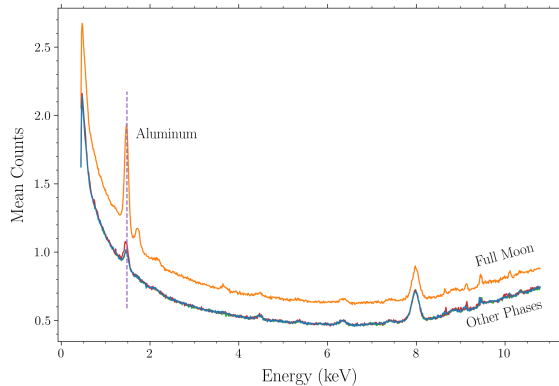


Figure: CLASS instrument (Source: Pillai et al. [13])

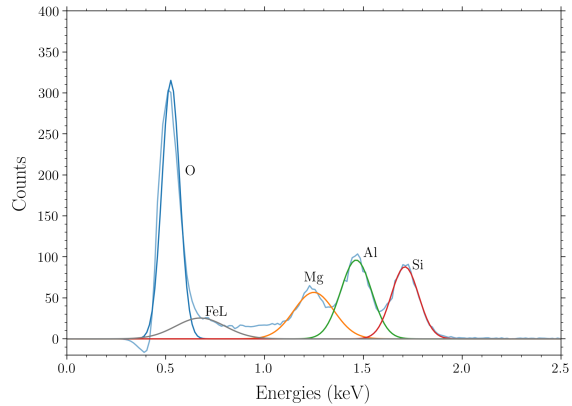
# METHODOLOGY

- » XRF detection using only CLASS data
  - Background model
  - Detection of elemental lines
- » Ratio between lines & uncertainties
  - Solar spectrum isn't needed, thus increasing overall data available
- » Mapping onto a lunar base map
- » Clustering, best ratios and compositional groups



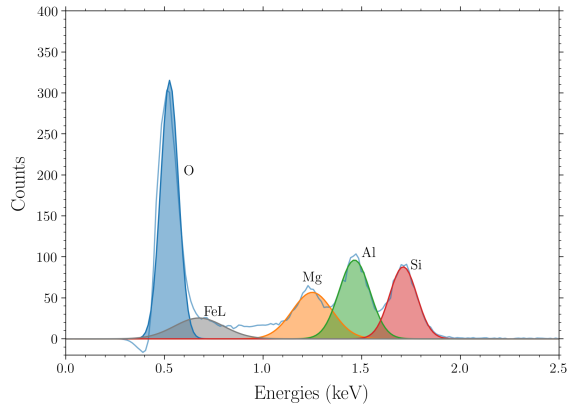
# METHODOLOGY

- » XRF detection using only CLASS data
  - Background model
  - Detection of elemental lines
- » Ratio between lines & uncertainties
  - Solar spectrum isn't needed, thus increasing overall data available
- » Mapping onto a lunar base map
- » Clustering, best ratios and compositional groups



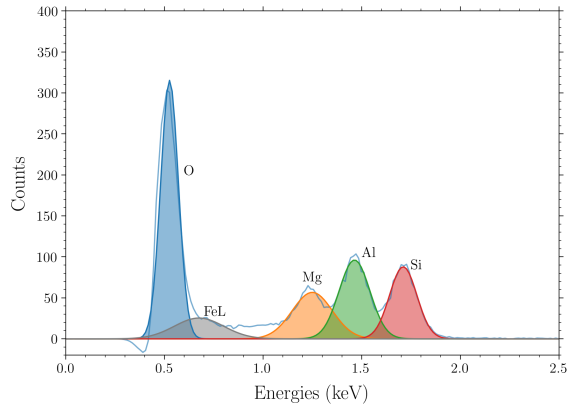
# METHODOLOGY

- » XRF detection using only CLASS data
  - Background model
  - Detection of elemental lines
- » Ratio between lines & uncertainties
  - Solar spectrum isn't needed, thus increasing overall data available
- » Mapping onto a lunar base map
- » Clustering, best ratios and compositional groups



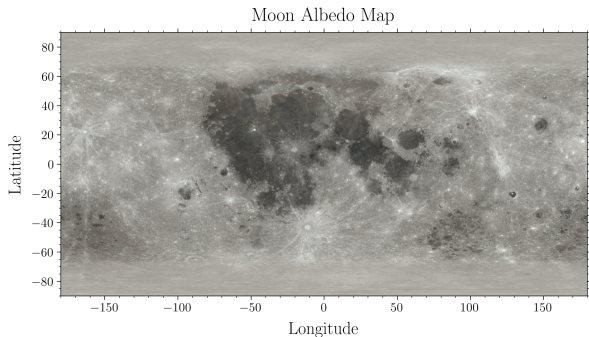
# METHODOLOGY

- » XRF detection using only CLASS data
  - Background model
  - Detection of elemental lines
- » Ratio between lines & uncertainties
  - Solar spectrum isn't needed, thus increasing overall data available
- » Mapping onto a lunar base map
- » Clustering, best ratios and compositional groups



# METHODOLOGY

- » XRF detection using only CLASS data
  - Background model
  - Detection of elemental lines
- » Ratio between lines & uncertainties
  - Solar spectrum isn't needed, thus increasing overall data available
- » Mapping onto a lunar base map
- » Clustering, best ratios and compositional groups



# METHODOLOGY

- » XRF detection using only CLASS data
  - Background model
  - Detection of elemental lines
- » Ratio between lines & uncertainties
  - Solar spectrum isn't needed, thus increasing overall data available
- » Mapping onto a lunar base map
- » Clustering, best ratios and compositional groups

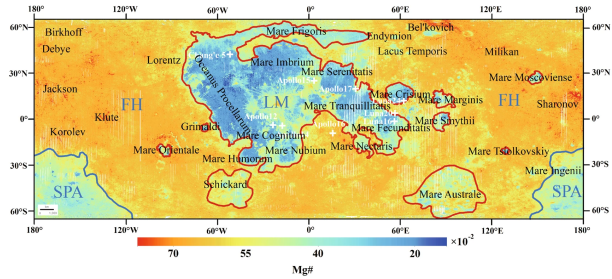


Figure: Source: Yang et al. [21]

# OUTLINE

---



## 1 Introduction

X-ray Fluorescence  
Methodology

## 2 XRF Detection

Algorithm  
L Transition Lines  
Results

## 3 Mapping

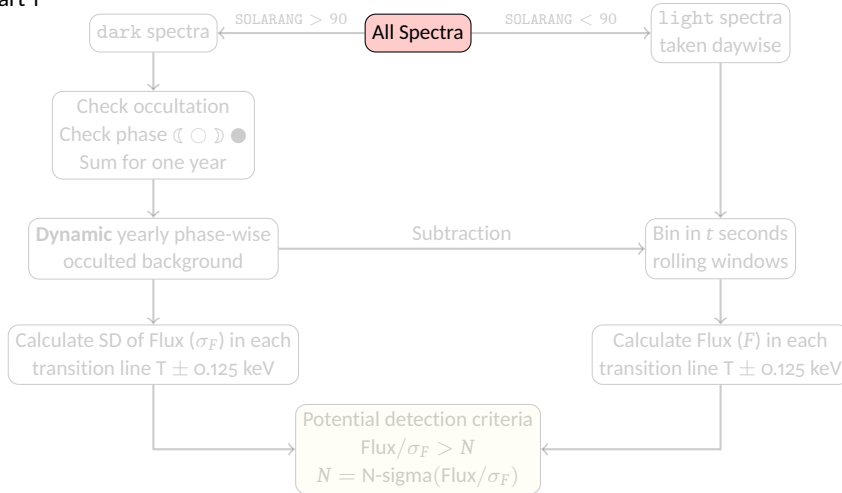
Methodology  
Results

## 4 Clustering

Ratio Selection  
1-D clustering  
2-D clustering

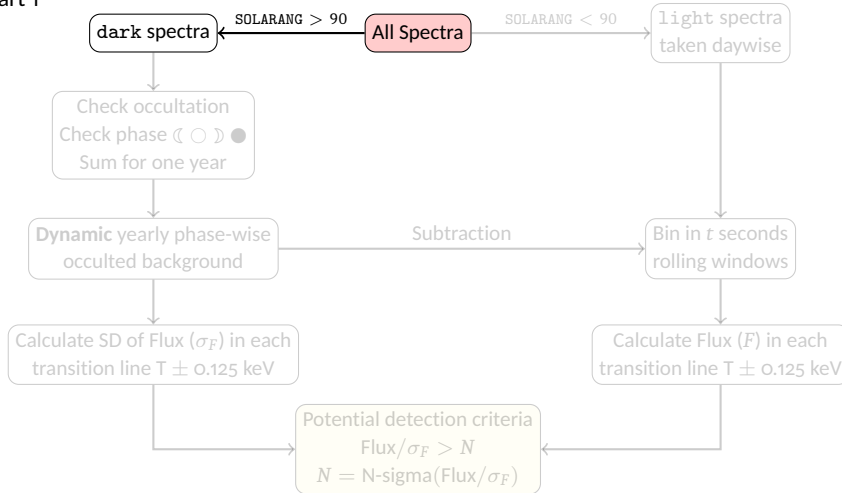
# DETECTION ALGORITHM

## Part 1



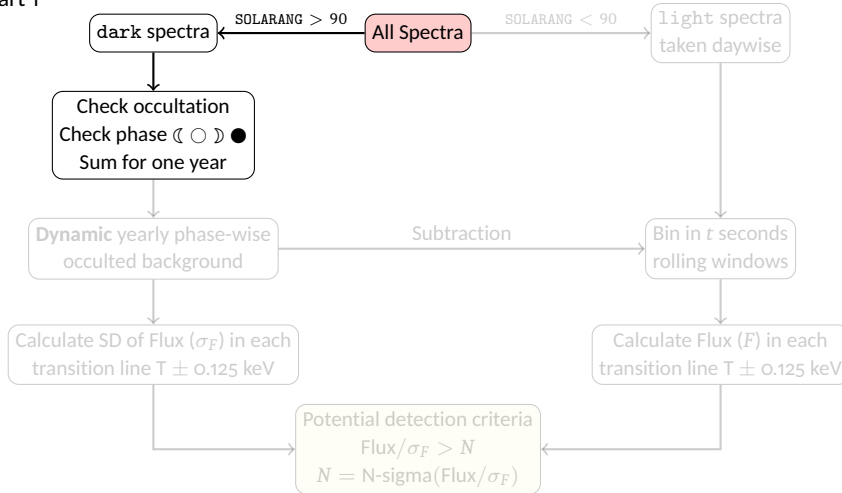
# DETECTION ALGORITHM

## Part 1



# DETECTION ALGORITHM

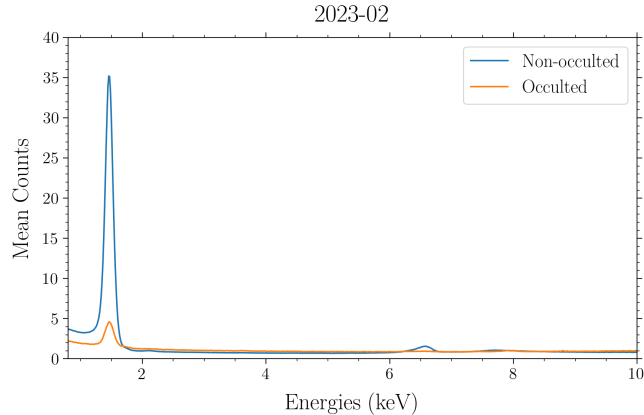
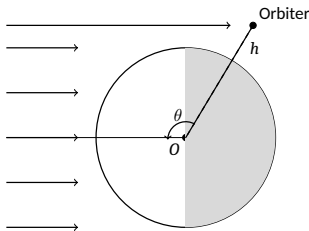
## Part 1



## DETECTION ALGORITHM

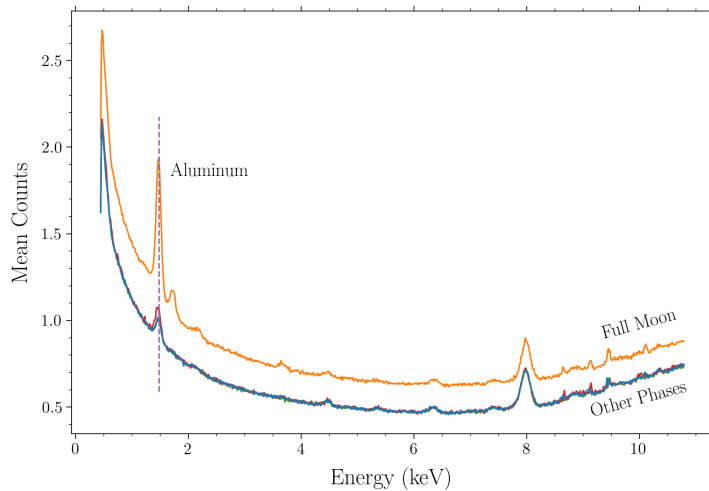


**Occultation** — Non-occulted backgrounds can cause oversubtraction of AI line!



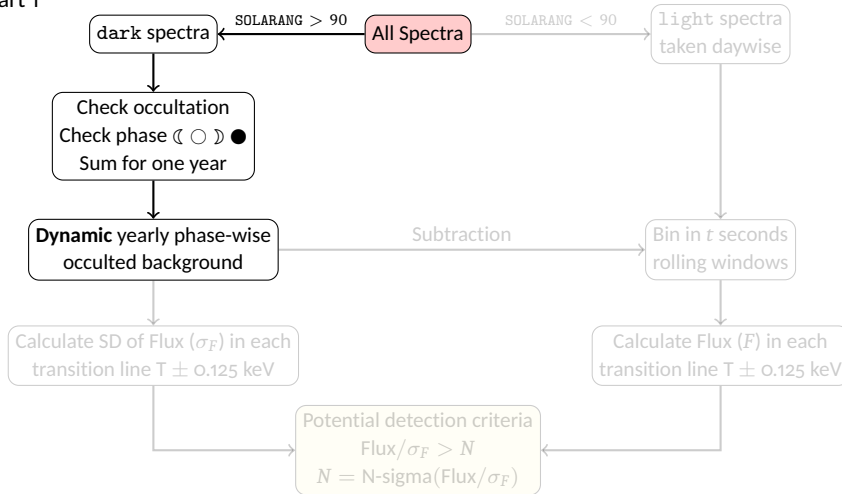
# DETECTION ALGORITHM

Geotail Effects — Adjusts background standard deviation according to phase



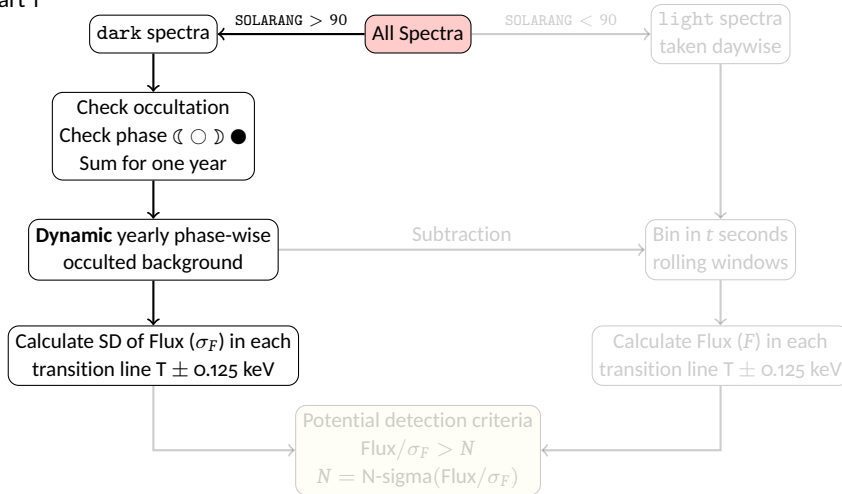
# DETECTION ALGORITHM

## Part 1



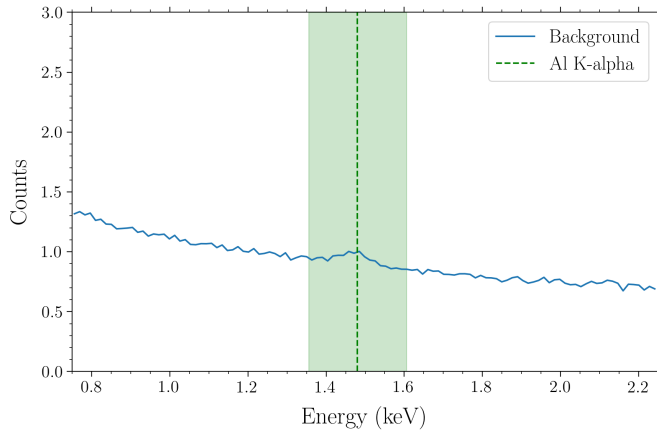
# DETECTION ALGORITHM

## Part 1



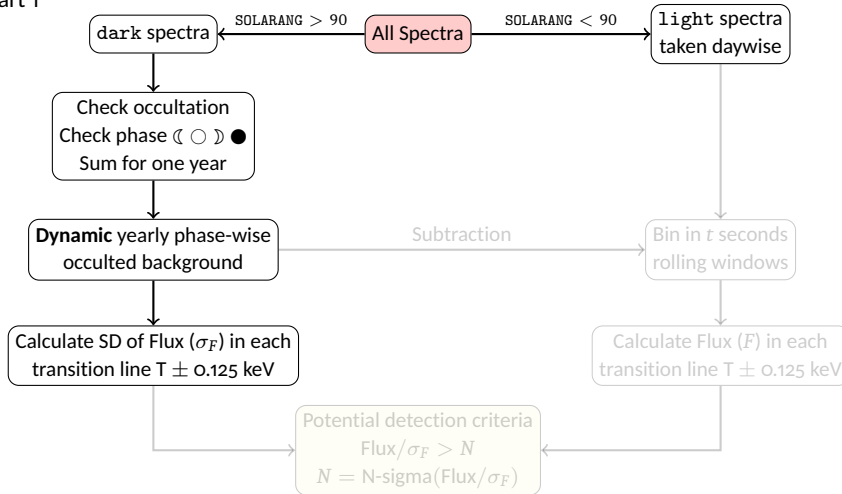
# DETECTION ALGORITHM

$E_{\text{K}-\alpha}^{\text{Al}} \pm 0.125 \text{ keV window}$



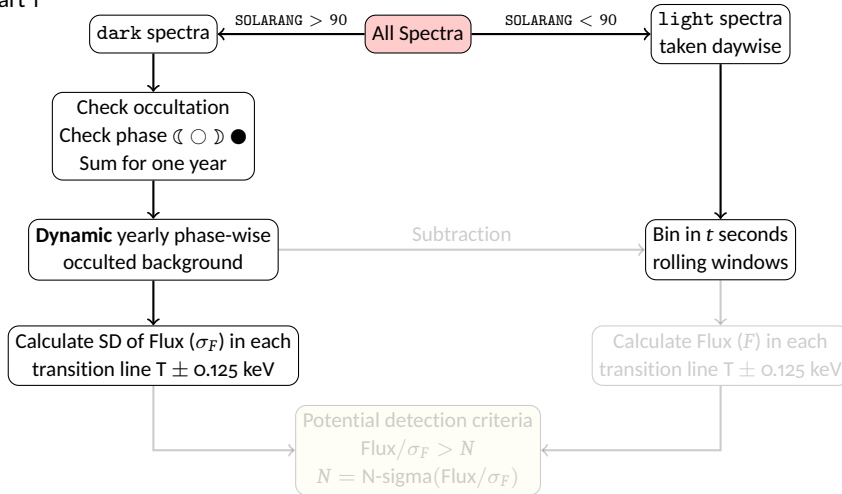
# DETECTION ALGORITHM

## Part 1



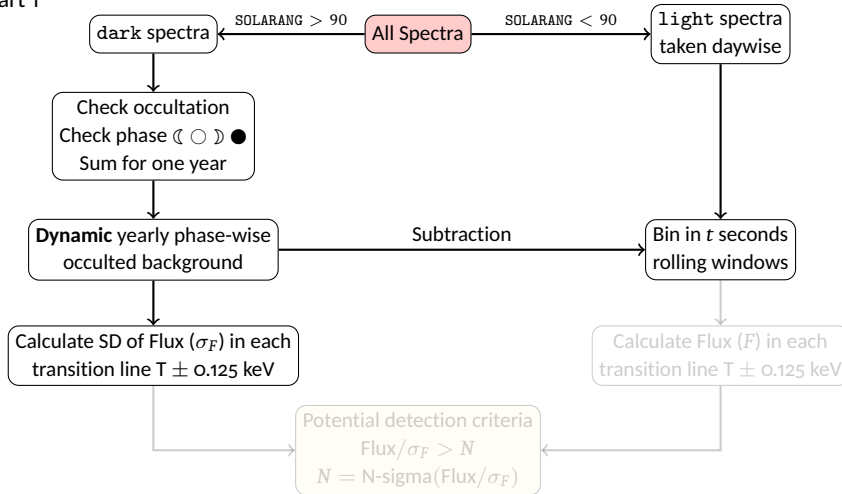
# DETECTION ALGORITHM

## Part 1



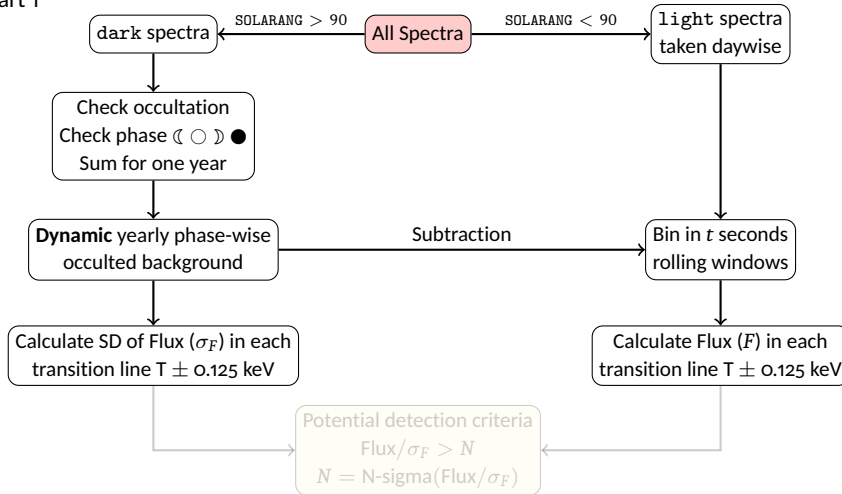
# DETECTION ALGORITHM

## Part 1



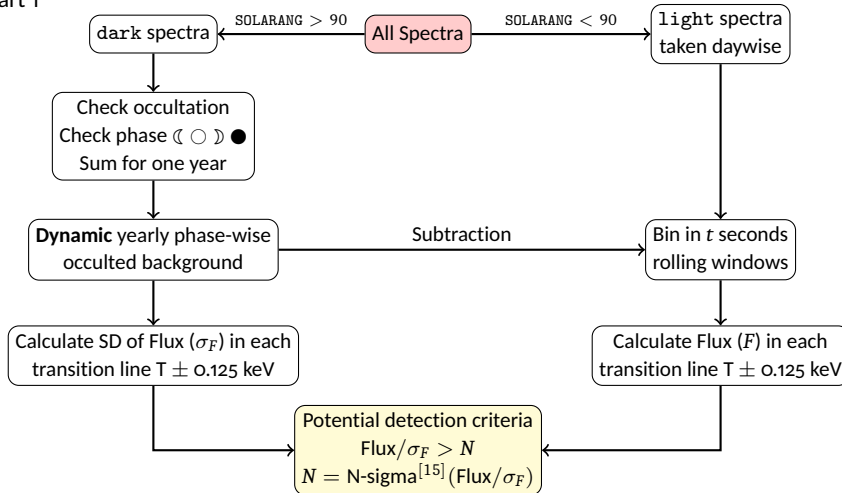
# DETECTION ALGORITHM

## Part 1



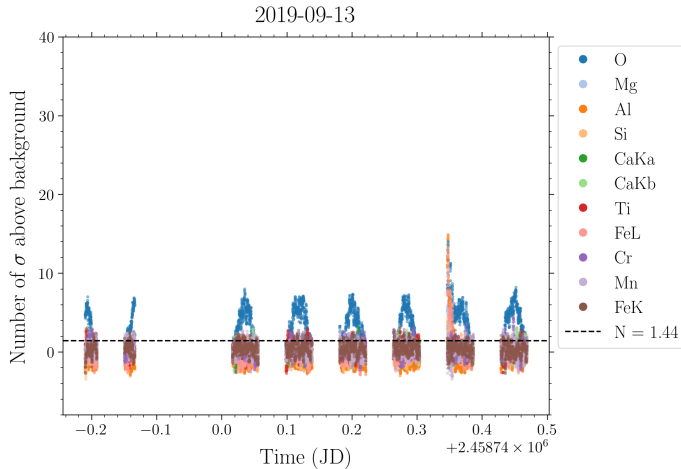
# DETECTION ALGORITHM

## Part 1



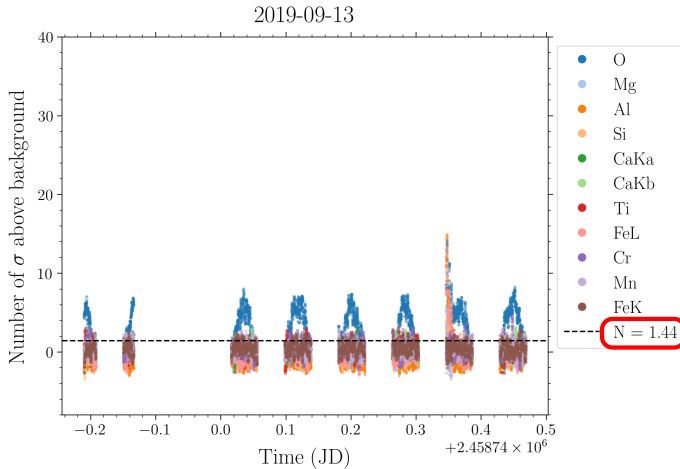
# DETECTION ALGORITHM

N-sigma — Low solar activity



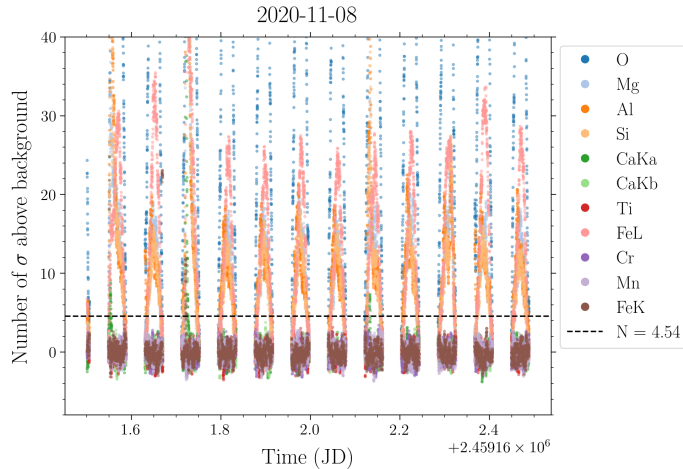
# DETECTION ALGORITHM

N-sigma — Low solar activity



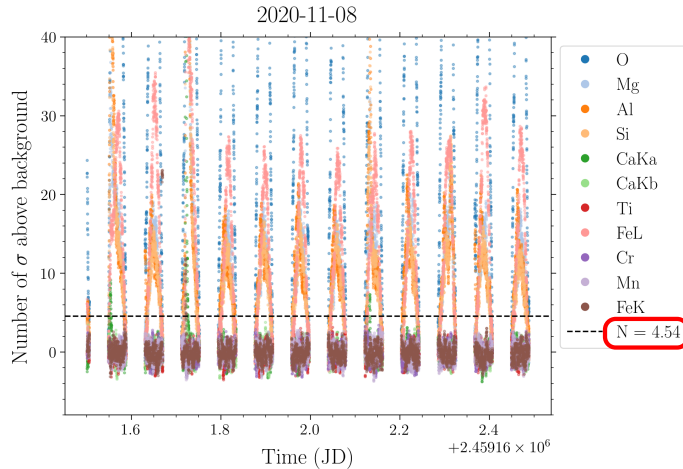
# DETECTION ALGORITHM

N-sigma — High solar activity



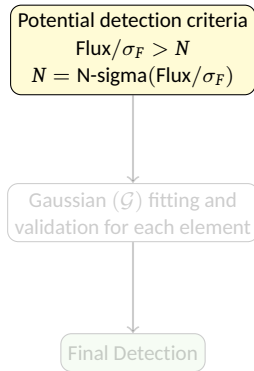
# DETECTION ALGORITHM

N-sigma — High solar activity



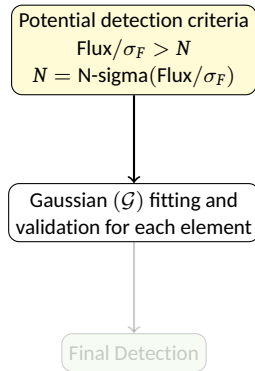
# DETECTION ALGORITHM

## Part 2



# DETECTION ALGORITHM

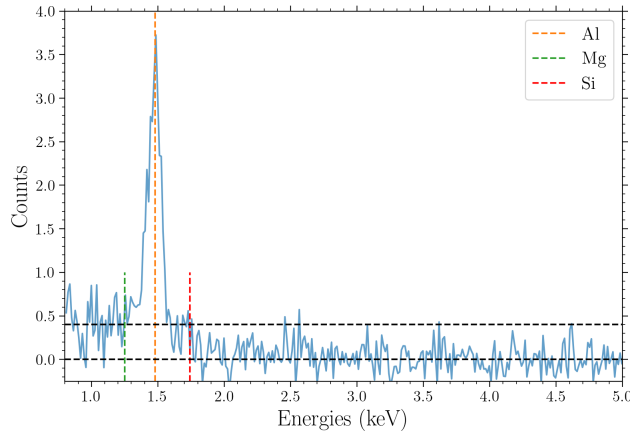
## Part 2



# DETECTION ALGORITHM

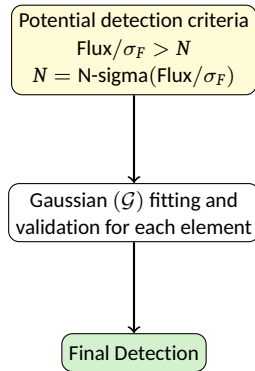
## Fit Validation

2019-11-13



# DETECTION ALGORITHM

## Part 2



# L TRANSITION LINES

- » Solar flare spectra are mostly in 1-2 keV range
- » Number of photons reduces exponentially with energy
- » K lines of Ca, Ti, Cr, Fe are very unlikely compared to L lines!
- » Ti, Cr line energies are too close to the large  $O_{K\alpha}$  line
- »  $Fe_L$  line is barely detectable

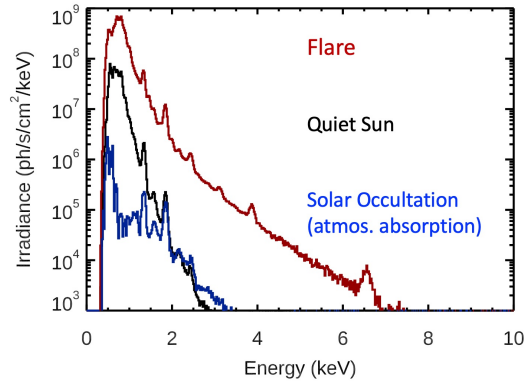


Figure: Solar Spectra (Source: Mason [11])

# L TRANSITION LINES

- » Solar flare spectra are mostly in 1-2 keV range
- » Number of photons reduces exponentially with energy
- » K lines of Ca, Ti, Cr, Fe are very unlikely compared to L lines!
- » Ti, Cr line energies are too close to the large  $O_{K\alpha}$  line
- »  $Fe_L$  line is barely detectable

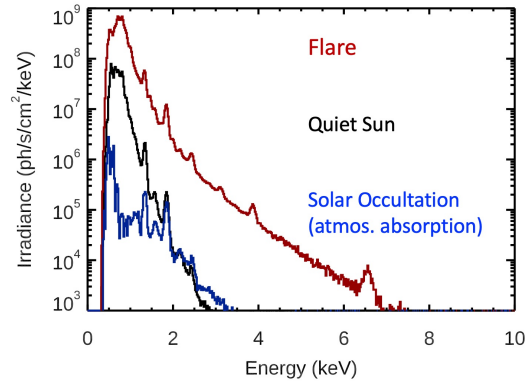


Figure: Solar Spectra (Source: Mason [11])

# L TRANSITION LINES

---

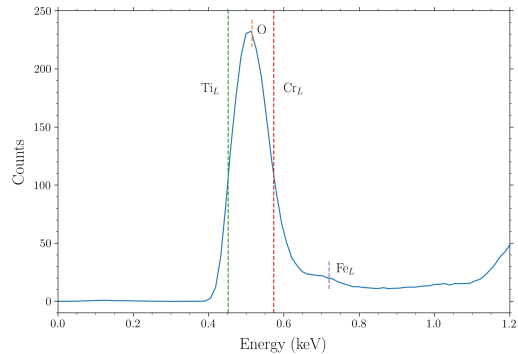


- » Solar flare spectra are mostly in 1-2 keV range
- » Number of photons reduces exponentially with energy
- » K lines of Ca, Ti, Cr, Fe are very unlikely compared to L lines!
- » Ti, Cr line energies are too close to the large  $O_{K\alpha}$  line
- »  $Fe_L$  line is barely detectable

Element	K shell (keV)	L shell (keV)
Ca	4	0.35
Ti	4.9	0.46
Cr	5.9	0.58
Fe	7.1	0.72

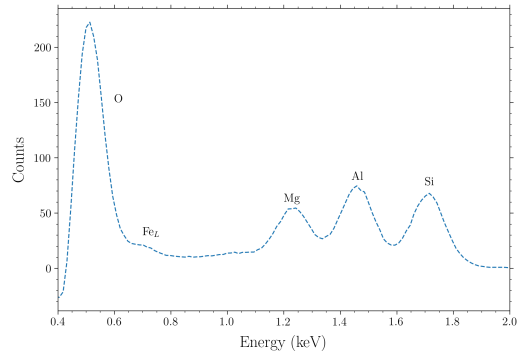
# L TRANSITION LINES

- » Solar flare spectra are mostly in 1-2 keV range
- » Number of photons reduces exponentially with energy
- » K lines of Ca, Ti, Cr, Fe are very unlikely compared to L lines!
- » Ti, Cr line energies are too close to the large  $O_{K\alpha}$  line
- »  $Fe_L$  line is barely detectable



# L TRANSITION LINES

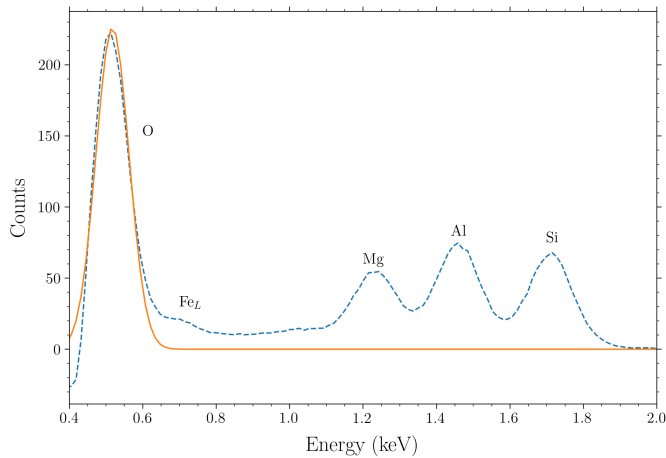
- » Solar flare spectra are mostly in 1-2 keV range
- » Number of photons reduces exponentially with energy
- » K lines of Ca, Ti, Cr, Fe are very unlikely compared to L lines!
- » Ti, Cr line energies are too close to the large  $O_{K\alpha}$  line
- »  $Fe_L$  line is barely detectable



# $\text{Fe}_L$ LINE METHODOLOGY

## Methodology

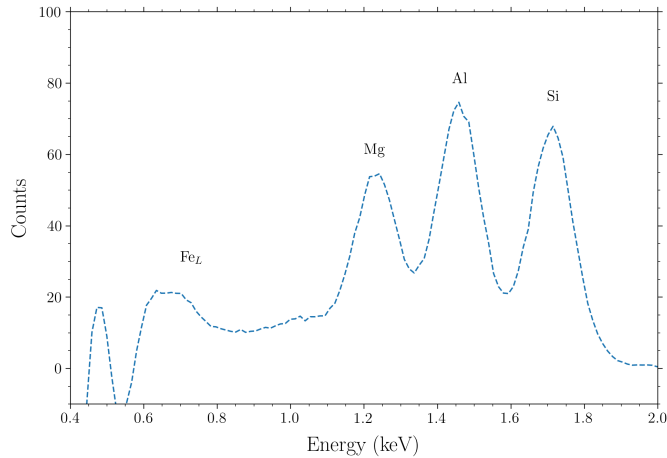
- » Fit single Gaussian to  $\text{O}_{\text{K}-\alpha}$  line
- » Subtract it from the spectrum
- » Fit single Gaussian to  $\text{Fe}_L$  line



# Fe<sub>L</sub> LINE METHODOLOGY

## Methodology

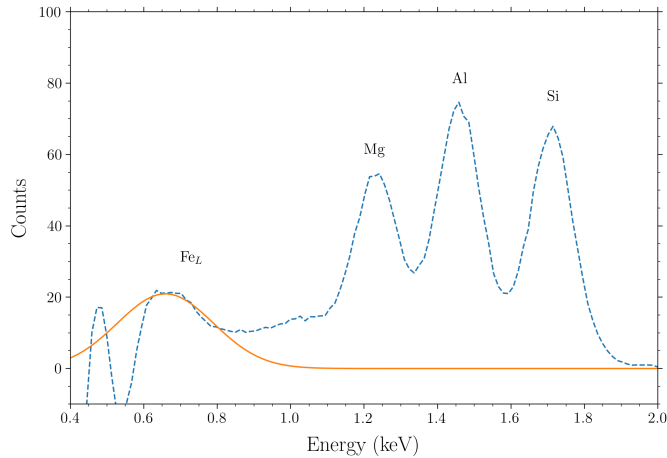
- » Fit single Gaussian to O<sub>K- $\alpha$</sub>  line
- » Subtract it from the spectrum
- » Fit single Gaussian to Fe<sub>L</sub> line



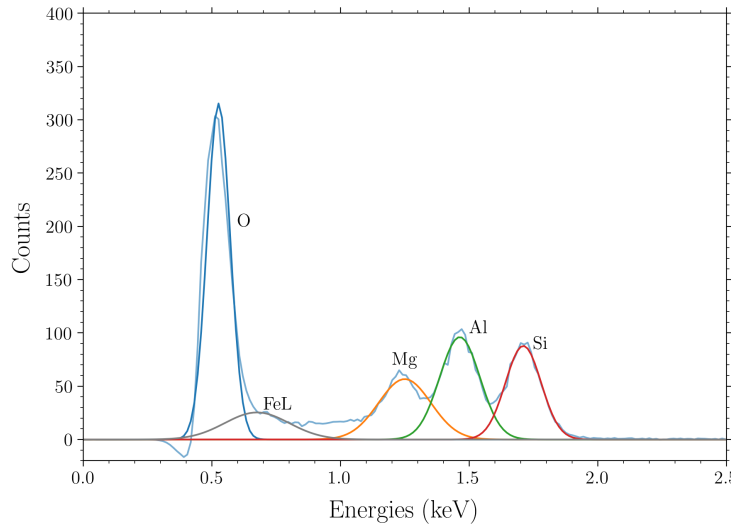
# $\text{Fe}_L$ LINE METHODOLOGY

## Methodology

- » Fit single Gaussian to  $\text{O}_{\text{K}-\alpha}$  line
- » Subtract it from the spectrum
- » Fit single Gaussian to  $\text{Fe}_L$  line



# RESULTS



# OUTLINE

---



## 1 Introduction

X-ray Fluorescence  
Methodology

## 2 XRF Detection

Algorithm  
L Transition Lines  
Results

## 3 Mapping

Methodology  
Results

## 4 Clustering

Ratio Selection  
1-D clustering  
2-D clustering

# METHODOLOGY

» We define the ratio  ${}^i\mathcal{R}_L^M$  of element  $M$  with element  $L$  for  $i^{\text{th}}$  observation in a pixel as:

$$» {}^i\mathcal{R}_L^M = \frac{A_M^i \sigma_M^i}{A_L^i \sigma_L^i} \quad (\text{Area under gaussian} = \sqrt{2\pi} A \sigma)$$

» Error ( $\Delta_i$ ) propagation using covariance matrix of the gaussian fits (p\_cov)

$$» {}^{\text{avg}}\mathcal{R}_L^M = \frac{\sum_{i=1}^n \frac{{}^i\mathcal{R}_L^M}{S_i \Delta_i^2}}{\sum_{i=1}^n \frac{1}{S_i \Delta_i^2}}, \quad \Delta({}^{\text{avg}}\mathcal{R}_L^M) = \frac{1}{\sqrt{\sum_{i=1}^n \frac{1}{S_i \Delta_i^2}}}, \quad \text{where } S_i \text{ is the area covered by the } 7^\circ \text{ FWHM}$$

# METHODOLOGY

» We define the ratio  ${}^i\mathcal{R}_L^M$  of element  $M$  with element  $L$  for  $i^{\text{th}}$  observation in a pixel as:

$$» {}^i\mathcal{R}_L^M = \frac{A_M^i \sigma_M^i}{A_L^i \sigma_L^i} \quad (\text{Area under gaussian} = \sqrt{2\pi} A \sigma)$$

» Error ( $\Delta_i$ ) propagation using covariance matrix of the gaussian fits (p\_cov)

$$» {}^{\text{avg}}\mathcal{R}_L^M = \frac{\sum_{i=1}^n \frac{{}^i\mathcal{R}_L^M}{S_i \Delta_i^2}}{\sum_{i=1}^n \frac{1}{S_i \Delta_i^2}}, \quad \Delta({}^{\text{avg}}\mathcal{R}_L^M) = \frac{1}{\sqrt{\sum_{i=1}^n \frac{1}{S_i \Delta_i^2}}}, \quad \text{where } S_i \text{ is the area covered by the } 7^\circ \text{ FWHM}$$

# METHODOLOGY

» We define the ratio  ${}^i\mathcal{R}_L^M$  of element  $M$  with element  $L$  for  $i^{\text{th}}$  observation in a pixel as:

$$» {}^i\mathcal{R}_L^M = \frac{A_M^i \sigma_M^i}{A_L^i \sigma_L^i} \quad (\text{Area under gaussian} = \sqrt{2\pi} A \sigma)$$

» Error ( $\Delta_i$ ) propagation using covariance matrix of the gaussian fits (p\_cov)

$$\» \text{avg } \mathcal{R}_L^M = \frac{\sum_{i=1}^n \frac{{}^i\mathcal{R}_L^M}{S_i \Delta_i^2}}{\sum_{i=1}^n \frac{1}{S_i \Delta_i^2}}, \quad \Delta(\text{avg } \mathcal{R}_L^M) = \frac{1}{\sqrt{\sum_{i=1}^n \frac{1}{S_i \Delta_i^2}}}, \quad \text{where } S_i \text{ is the area covered by the } 7^\circ \text{ FWHM}$$

# METHODOLOGY

» We define the ratio  ${}^i\mathcal{R}_L^M$  of element  $M$  with element  $L$  for  $i^{\text{th}}$  observation in a pixel as:

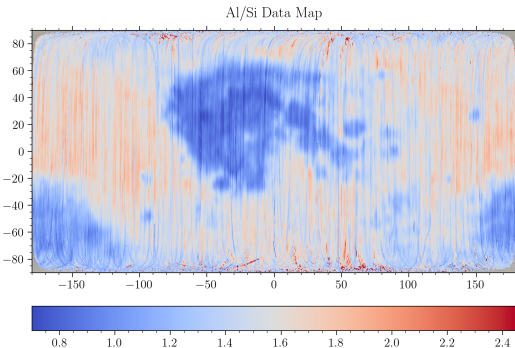
$$» {}^i\mathcal{R}_L^M = \frac{A_M^i \sigma_M^i}{A_L^i \sigma_L^i} \quad (\text{Area under gaussian} = \sqrt{2\pi} A \sigma)$$

» Error ( $\Delta_i$ ) propagation using covariance matrix of the gaussian fits (p\_cov)

$$» {}^{\text{avg}}\mathcal{R}_L^M = \frac{\sum_{i=1}^n \frac{{}^i\mathcal{R}_L^M}{S_i \Delta_i^2}}{\sum_{i=1}^n \frac{1}{S_i \Delta_i^2}}, \quad \Delta({}^{\text{avg}}\mathcal{R}_L^M) = \frac{1}{\sqrt{\sum_{i=1}^n \frac{1}{S_i \Delta_i^2}}}, \quad \text{where } S_i \text{ is the area covered by the } 7^\circ \text{ FWHM}$$

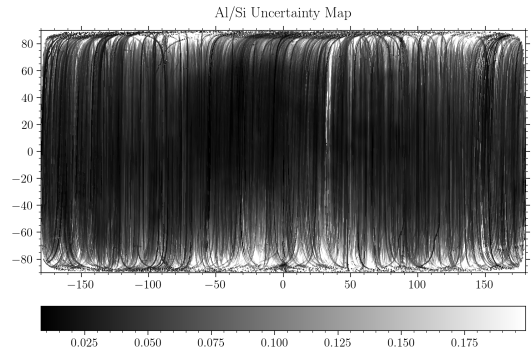
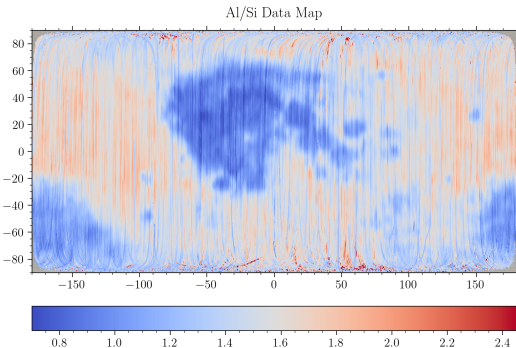
# RESULTS

$\mathcal{R}_{\text{Si}}^{\text{Al}}$  — 96 s binning



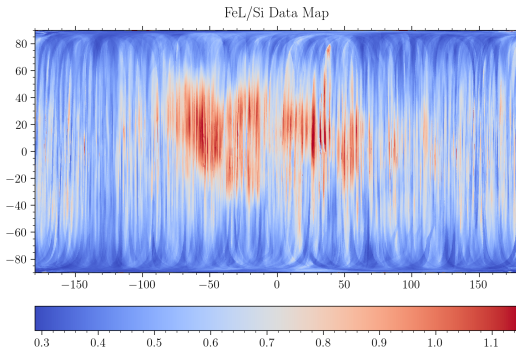
# RESULTS

$\mathcal{R}_{\text{Si}}^{\text{Al}}$  — 96 s binning



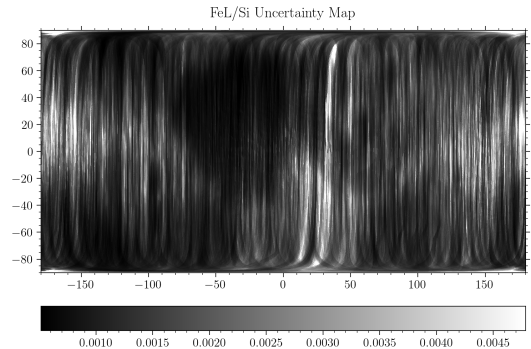
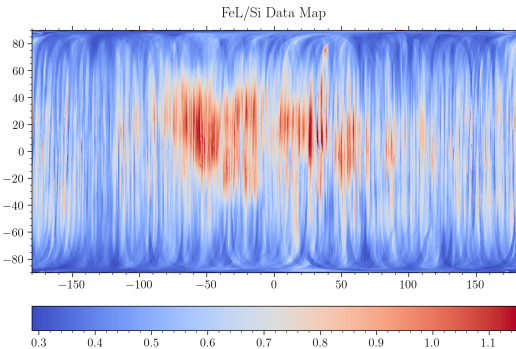
# RESULTS

$\mathcal{R}_{\text{Si}}^{\text{FeL}} - 296 \text{ s binning}$



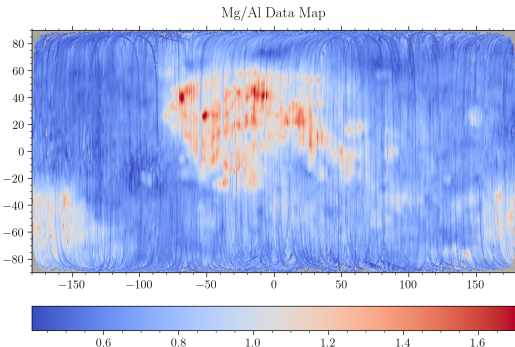
# RESULTS

$\mathcal{R}_{\text{Si}}^{\text{FeL}} - 296 \text{ s binning}$



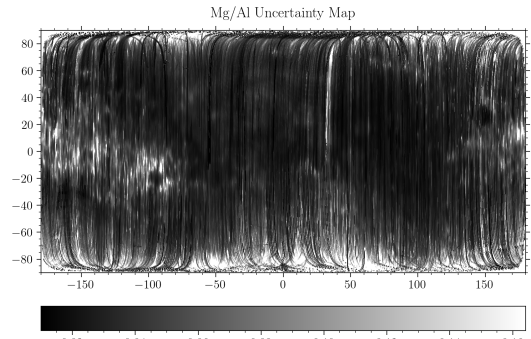
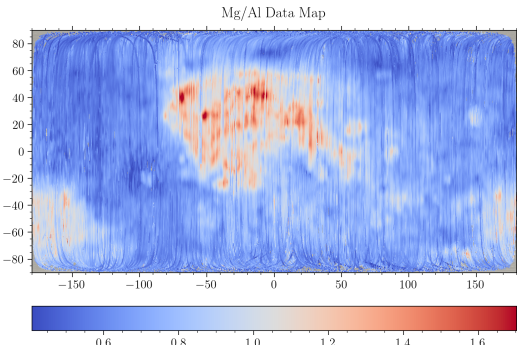
# RESULTS

$\mathcal{R}_{\text{Al}}^{\text{Mg}}$  — 96 s binning



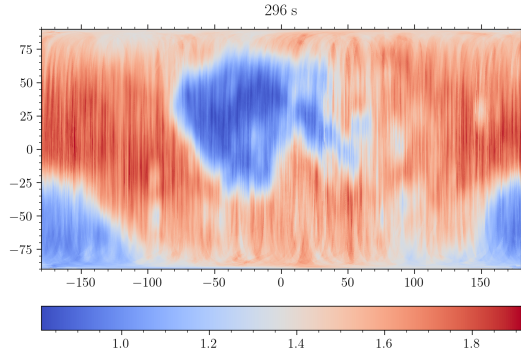
# RESULTS

$\mathcal{R}_{\text{Al}}^{\text{Mg}} - 96 \text{ s binning}$



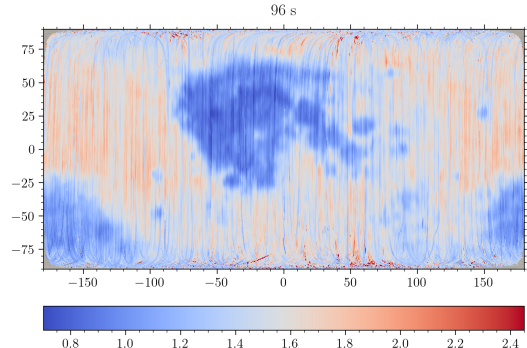
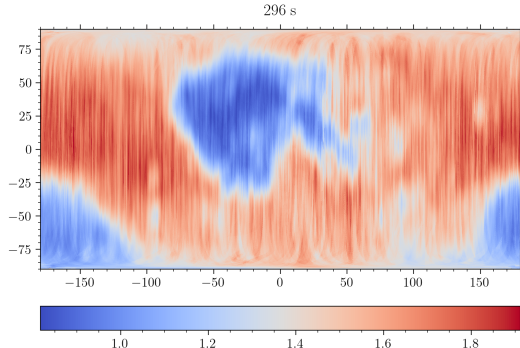
# TIME BIN VS RESOLUTION

$\mathcal{R}_{\text{Si}}^{\text{AI}}$  map comparison between 296 s and 96 s binning



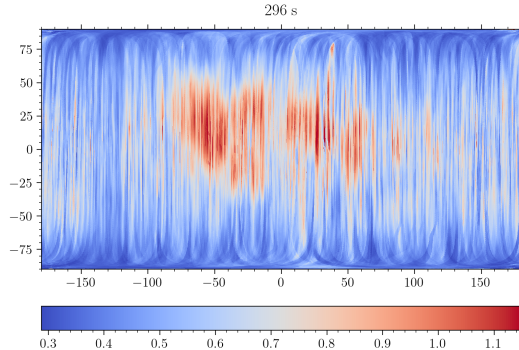
# TIME BIN VS RESOLUTION

$\mathcal{R}_{\text{Si}}^{\text{AI}}$  map comparison between 296 s and 96 s binning



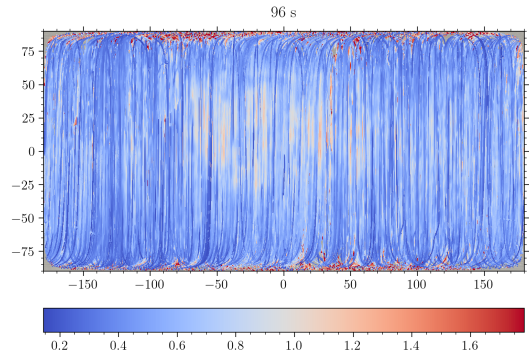
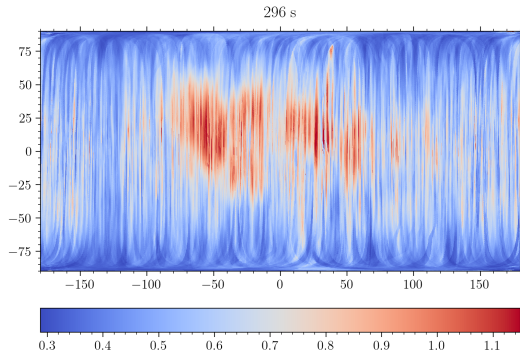
# TIME BIN VS RESOLUTION

$\mathcal{R}_{\text{Si}}^{\text{Fe}}$  map comparison between 296 s and 96 s binning



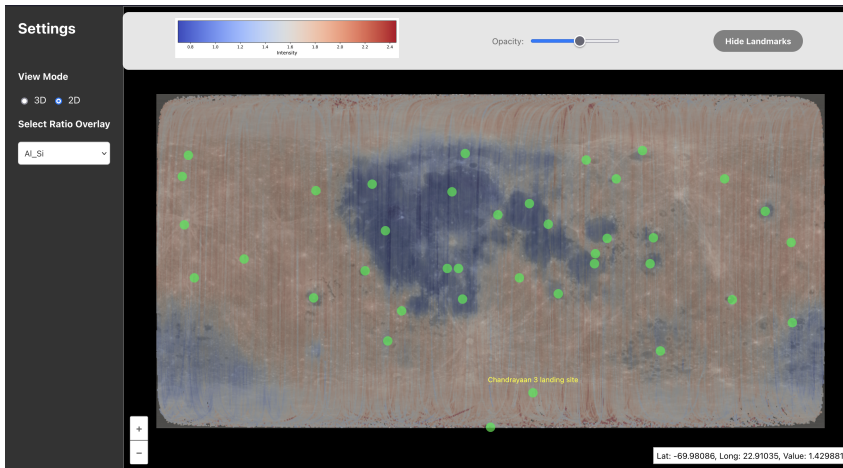
# TIME BIN VS RESOLUTION

$\mathcal{R}_{\text{Si}}^{\text{Fe}}$  map comparison between 296 s and 96 s binning



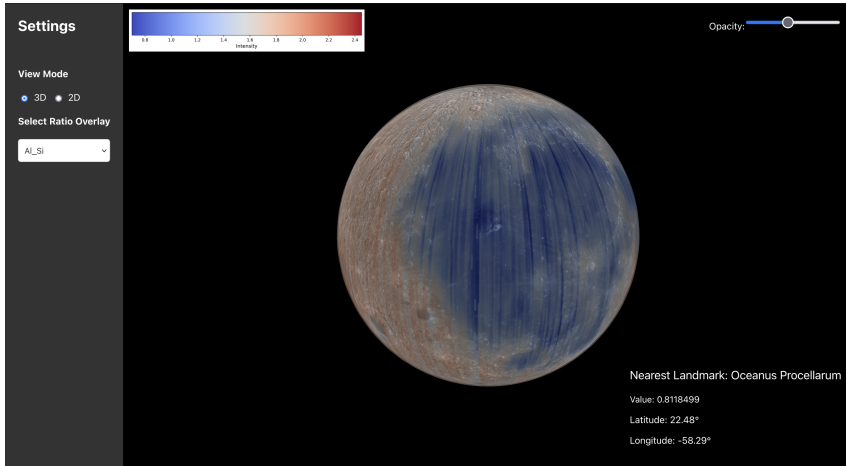
# VISUALIZATION TOOL

React based 2-D and 3-D interactive TIFF viewer



# VISUALIZATION TOOL

React based 2-D and 3-D interactive TIFF viewer



# OUTLINE

---



## 1 Introduction

X-ray Fluorescence  
Methodology

## 2 XRF Detection

Algorithm  
L Transition Lines  
Results

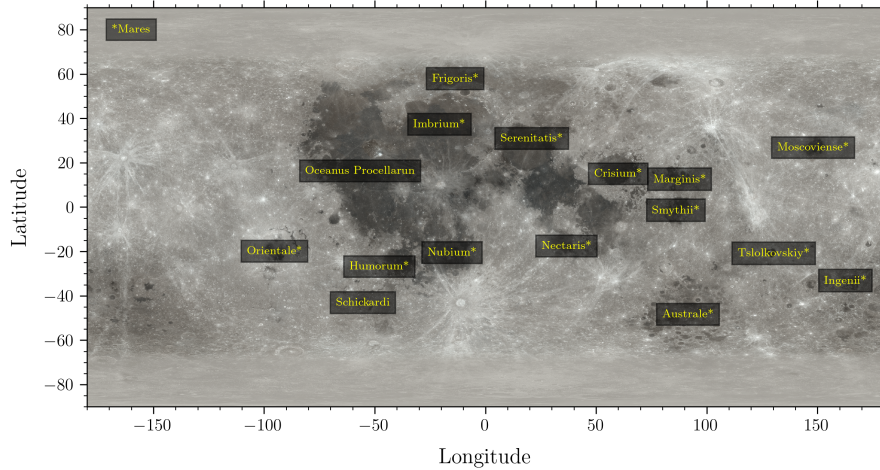
## 3 Mapping

Methodology  
Results

## 4 Clustering

Ratio Selection  
1-D clustering  
2-D clustering

# SELENOGRAPHICAL MAP



# SELECTION OF RATIOS

- » Taking elemental ratios with Silicon is convenient due to its constant ( $45\% \pm 10\%$ ) composition and high abundance.
- » **Composite Ratios:** Taking combination of individual ratios —  $Mg\# = \frac{MgO}{MgO + FeO} \mid \frac{\mathcal{R}_{Si}^{Mg}}{\mathcal{R}_{Si}^{Mg} + \mathcal{R}_{Si}^{Fe}}$
- » **1-D Clustering:** Taking histograms individually ( $\mathcal{R}_{Si}^{Al}$ ,  $\mathcal{R}_{Si}^{Mg}$ , Mg#). The limited dimensionality collapses clusters.
- » **2-D Clustering:** Taking pairs of individual ratios ( $[\mathcal{R}_{Al}^{Mg}, \mathcal{R}_{Si}^{Al}]$ ,  $[\mathcal{R}_{Si}^{Fe}, \mathcal{R}_{Si}^{Al}]$ ) to make correlation plots reveals information about both elements.

We validate known results and go further than previous research on line ratios using our novel 2-D clustering approach.

# SELECTION OF RATIOS



- » Taking elemental ratios with Silicon is convenient due to its constant ( $45\% \pm 10\%$ ) composition and high abundance.
- » **Composite Ratios:** Taking combination of individual ratios —  $Mg\# = \frac{MgO}{MgO + FeO} \mid \frac{\mathcal{R}_{Si}^{Mg}}{\mathcal{R}_{Si}^{Mg} + \mathcal{R}_{Si}^{Fe}}$
- » **1-D Clustering:** Taking histograms individually ( $\mathcal{R}_{Si}^{Al}$ ,  $\mathcal{R}_{Si}^{Mg}$ , Mg#). The limited dimensionality collapses clusters.
- » **2-D Clustering:** Taking pairs of individual ratios ( $[\mathcal{R}_{Al}^{Mg}, \mathcal{R}_{Si}^{Al}]$ ,  $[\mathcal{R}_{Si}^{Fe}, \mathcal{R}_{Si}^{Al}]$ ) to make correlation plots reveals information about both elements.

We validate known results and go further than previous research on line ratios using our novel 2-D clustering approach.

# SELECTION OF RATIOS



- » Taking elemental ratios with Silicon is convenient due to its constant ( $45\% \pm 10\%$ ) composition and high abundance.
- » **Composite Ratios:** Taking combination of individual ratios —  $Mg\# = \frac{MgO}{MgO + FeO} \mid \frac{\mathcal{R}_{Si}^{Mg}}{\mathcal{R}_{Si}^{Mg} + \mathcal{R}_{Si}^{Fe}}$
- » **1-D Clustering:** Taking histograms individually ( $\mathcal{R}_{Si}^{Al}$ ,  $\mathcal{R}_{Si}^{Mg}$ , Mg#). The limited dimensionality collapses clusters.
- » **2-D Clustering:** Taking pairs of individual ratios ( $[\mathcal{R}_{Al}^{Mg}, \mathcal{R}_{Si}^{Al}]$ ,  $[\mathcal{R}_{Si}^{Fe}, \mathcal{R}_{Si}^{Al}]$ ) to make correlation plots reveals information about both elements.

We validate known results and go further than previous research on line ratios using our novel 2-D clustering approach.

# SELECTION OF RATIOS

- » Taking elemental ratios with Silicon is convenient due to its constant ( $45\% \pm 10\%$ ) composition and high abundance.
- » **Composite Ratios:** Taking combination of individual ratios —  $Mg\# = \frac{MgO}{MgO + FeO} \mid \frac{\mathcal{R}_{Si}^{Mg}}{\mathcal{R}_{Si}^{Mg} + \mathcal{R}_{Si}^{Fe}}$
- » **1-D Clustering:** Taking histograms individually ( $\mathcal{R}_{Si}^{Al}$ ,  $\mathcal{R}_{Si}^{Mg}$ , Mg#). The limited dimensionality collapses clusters.
- » **2-D Clustering:** Taking pairs of individual ratios ( $[\mathcal{R}_{Al}^{Mg}, \mathcal{R}_{Si}^{Al}]$ ,  $[\mathcal{R}_{Si}^{Fe}, \mathcal{R}_{Si}^{Al}]$ ) to make correlation plots reveals information about both elements.

We validate known results and go further than previous research on line ratios using our novel 2-D clustering approach.

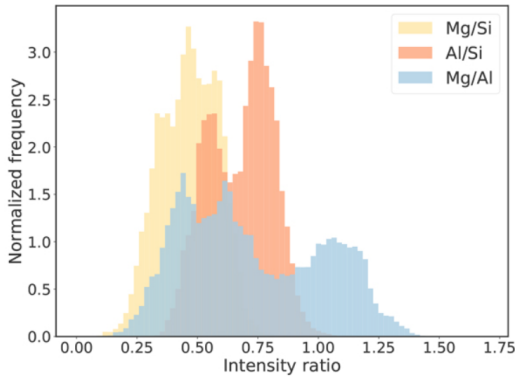
# SELECTION OF RATIOS

- » Taking elemental ratios with Silicon is convenient due to its constant ( $45\% \pm 10\%$ ) composition and high abundance.
- » **Composite Ratios:** Taking combination of individual ratios —  $Mg\# = \frac{MgO}{MgO + FeO} \mid \frac{\mathcal{R}_{Si}^{Mg}}{\mathcal{R}_{Si}^{Mg} + \mathcal{R}_{Si}^{Fe}}$
- » **1-D Clustering:** Taking histograms individually ( $\mathcal{R}_{Si}^{Al}$ ,  $\mathcal{R}_{Si}^{Mg}$ , Mg#). The limited dimensionality collapses clusters.
- » **2-D Clustering:** Taking pairs of individual ratios ( $[\mathcal{R}_{Al}^{Mg}, \mathcal{R}_{Si}^{Al}]$ ,  $[\mathcal{R}_{Si}^{Fe}, \mathcal{R}_{Si}^{Al}]$ ) to make correlation plots reveals information about both elements.

We validate known results and go further than previous research on line ratios using our novel 2-D clustering approach.

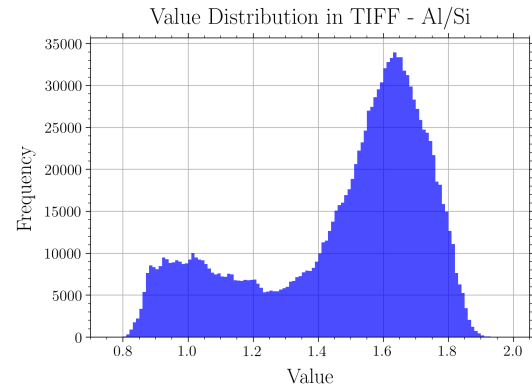
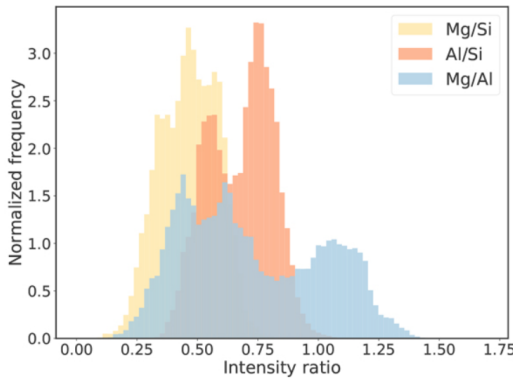
# 1-D RATIO CLUSTERS

$\mathcal{R}_{\text{Si}}^{\text{Al}}$  — Comparison of histogram with Apollo 15/16 Gloudemans, A. J. et al. [8]



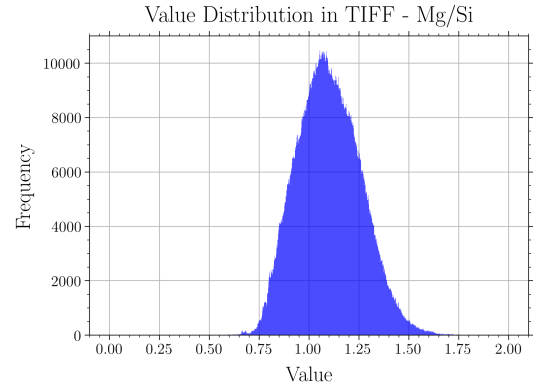
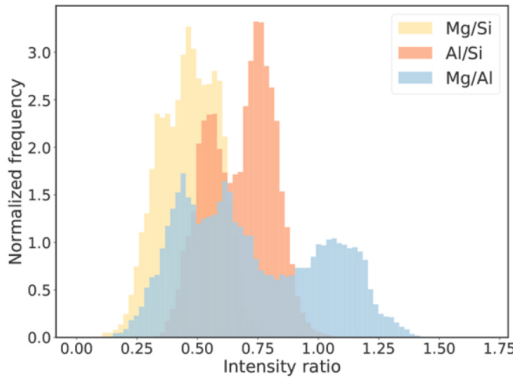
# 1-D RATIO CLUSTERS

$\mathcal{R}_{\text{Si}}^{\text{Al}}$  – Comparison of histogram with Apollo 15/16 Gloudemans, A. J. et al. [8]



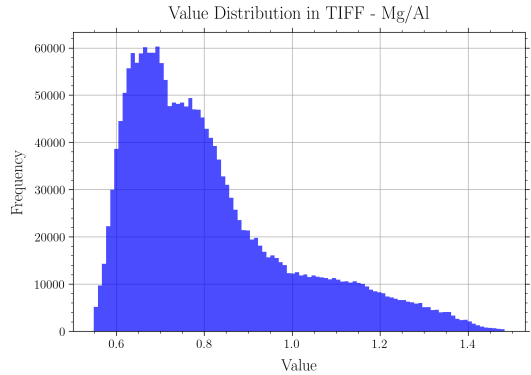
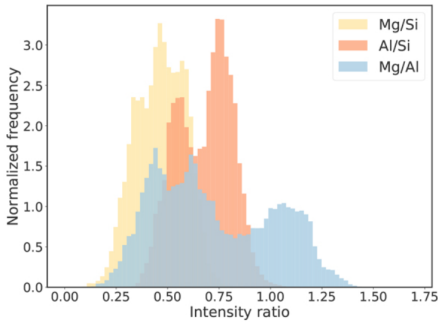
# 1-D RATIO CLUSTERS

$\mathcal{R}_{\text{Si}}^{\text{Mg}}$  — Comparison of histogram with Apollo 15/16 Gloudemans, A. J. et al. [8]



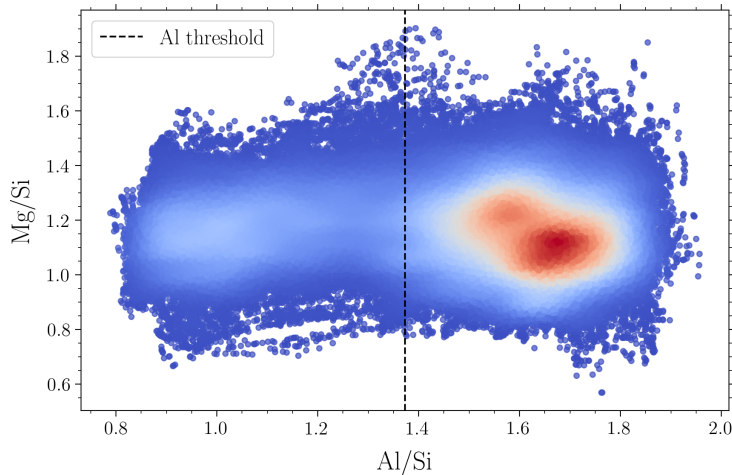
# 1-D RATIO CLUSTERS

$\mathcal{R}_{\text{Al}}^{\text{Mg}}$  — Comparison of histogram with Apollo 15/16 Gloudemans, A. J. et al. [8]



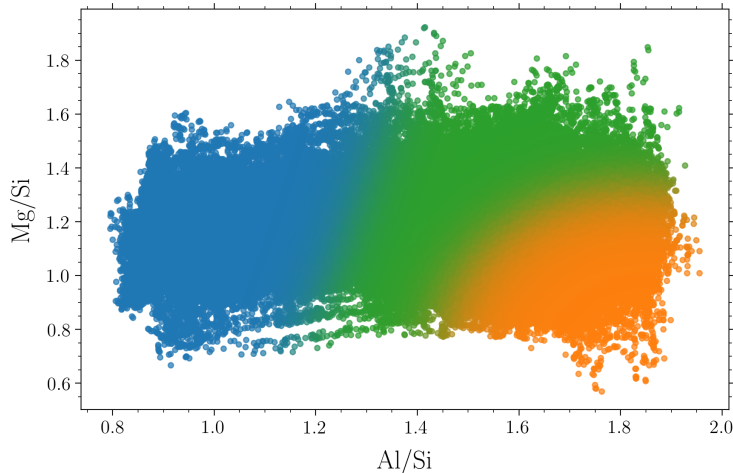
# 2-D RATIO CLUSTERS

$\mathcal{R}_{\text{Si}}^{\text{Al}}$  and  $\mathcal{R}_{\text{Si}}^{\text{Mg}}$  — Density Plot



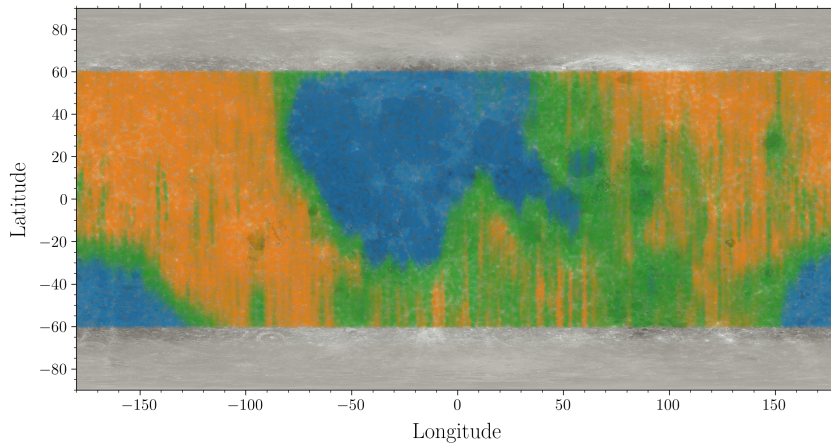
## 2-D RATIO CLUSTERS

$\mathcal{R}_{\text{Si}}^{\text{Al}}$  and  $\mathcal{R}_{\text{Si}}^{\text{Mg}}$  — Three GMM



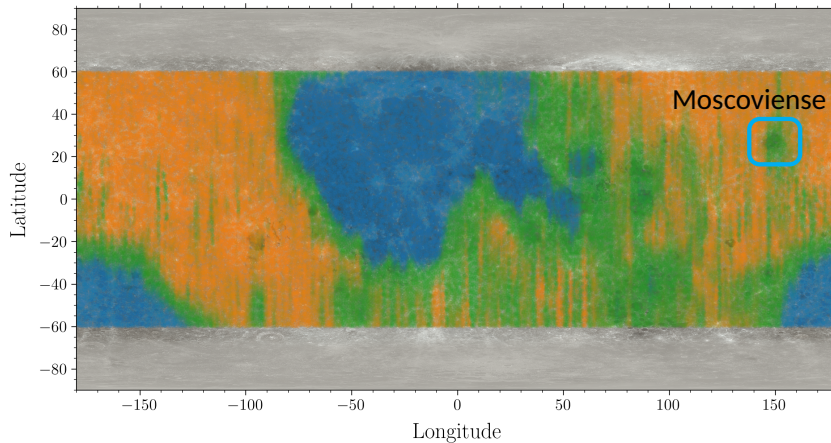
# 2-D RATIO CLUSTERS

$\mathcal{R}_{\text{Si}}^{\text{Al}}$  and  $\mathcal{R}_{\text{Si}}^{\text{Mg}}$  — Cluster Visualization



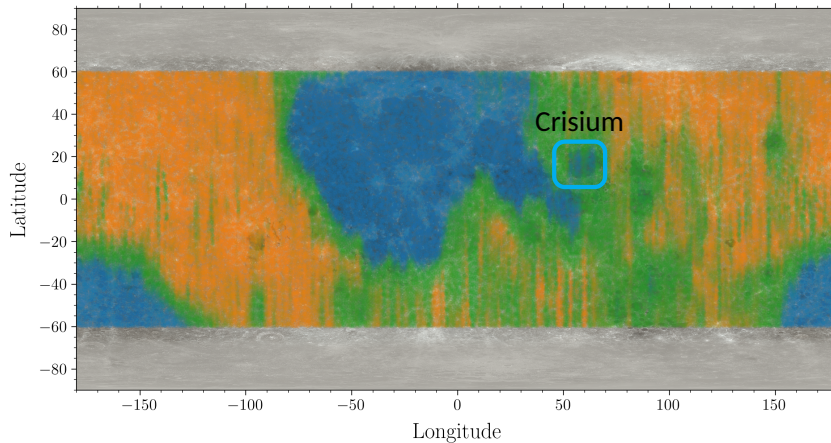
# 2-D RATIO CLUSTERS

$\mathcal{R}_{\text{Si}}^{\text{Al}}$  and  $\mathcal{R}_{\text{Si}}^{\text{Mg}}$  — Cluster Visualization



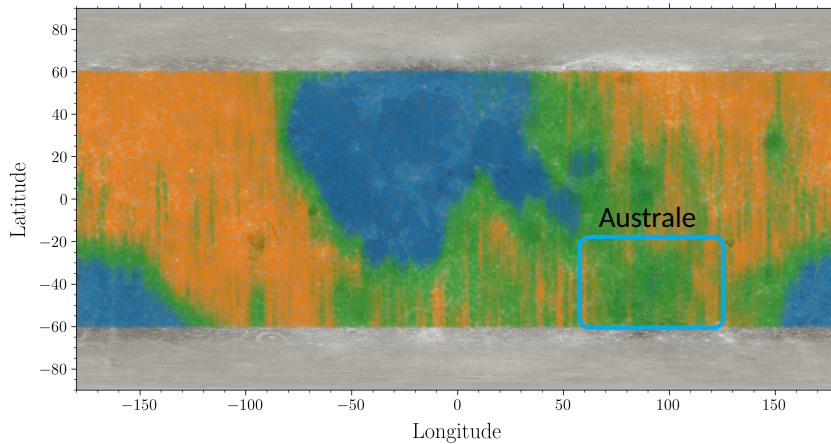
# 2-D RATIO CLUSTERS

$\mathcal{R}_{\text{Si}}^{\text{Al}}$  and  $\mathcal{R}_{\text{Si}}^{\text{Mg}}$  — Cluster Visualization



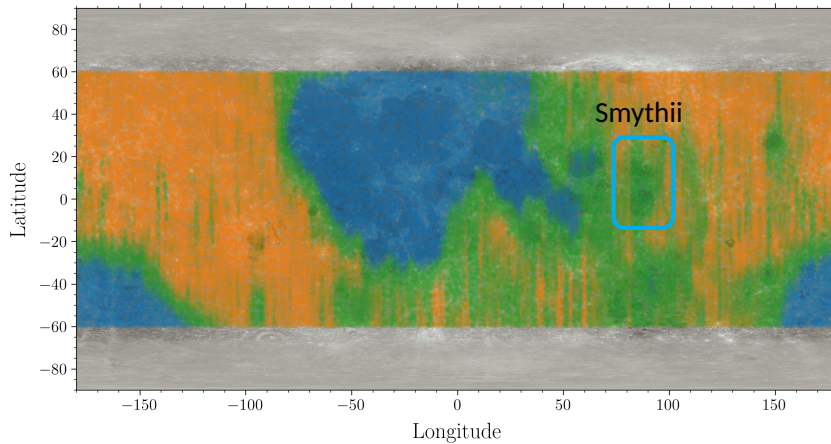
# 2-D RATIO CLUSTERS

$\mathcal{R}_{\text{Si}}^{\text{Al}}$  and  $\mathcal{R}_{\text{Si}}^{\text{Mg}}$  — Cluster Visualization



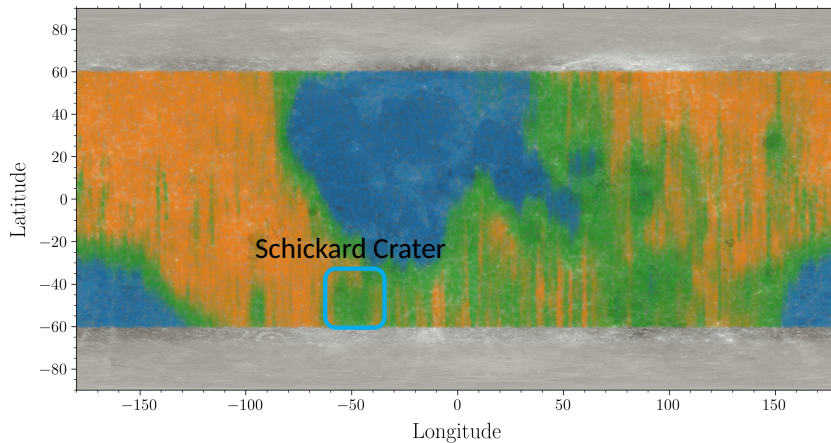
# 2-D RATIO CLUSTERS

$\mathcal{R}_{\text{Si}}^{\text{Al}}$  and  $\mathcal{R}_{\text{Si}}^{\text{Mg}}$  — Cluster Visualization



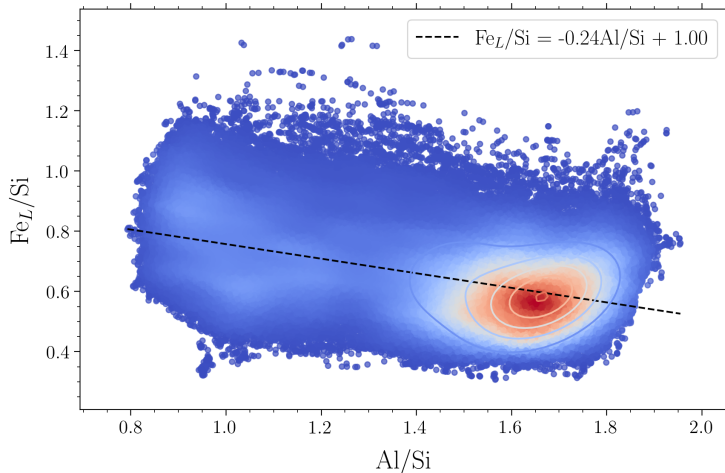
# 2-D RATIO CLUSTERS

$\mathcal{R}_{\text{Si}}^{\text{Al}}$  and  $\mathcal{R}_{\text{Si}}^{\text{Mg}}$  — Cluster Visualization



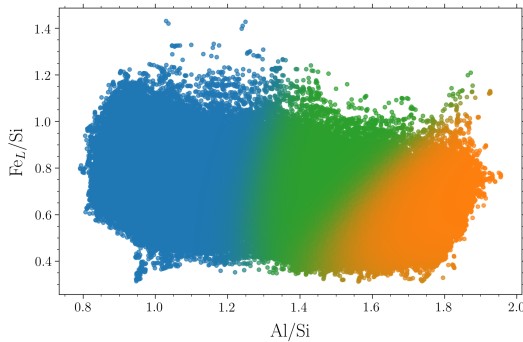
## 2-D RATIO CLUSTERS

$\mathcal{R}_{\text{Si}}^{\text{Al}}$  and  $\mathcal{R}_{\text{Si}}^{\text{Fe}}$  — Density Plot



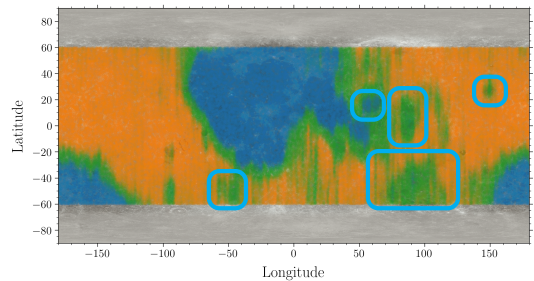
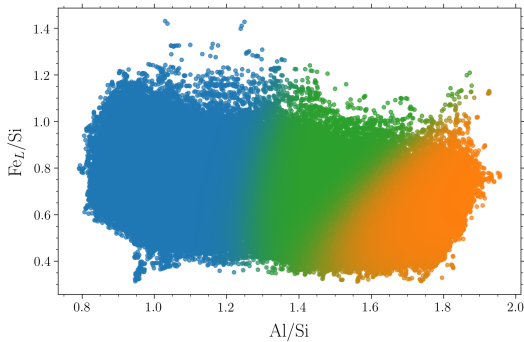
## 2-D RATIO CLUSTERS

$\mathcal{R}_{\text{Si}}^{\text{Al}}$  vs  $\mathcal{R}_{\text{Si}}^{\text{Fe}}$  — Clusters in composition space and real space



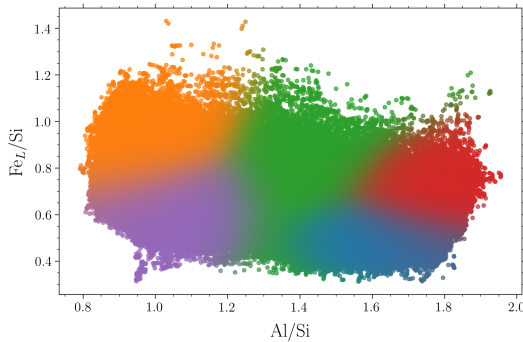
## 2-D RATIO CLUSTERS

$\mathcal{R}_{\text{Si}}^{\text{Al}}$  vs  $\mathcal{R}_{\text{Si}}^{\text{Fe}}$  — Clusters in composition space and real space



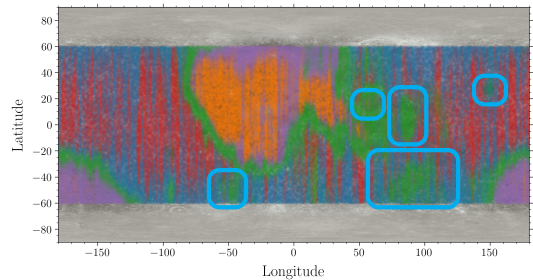
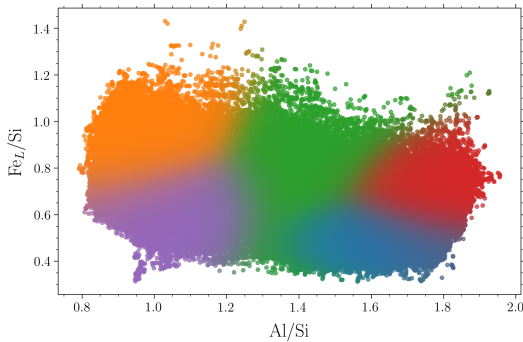
## 2-D RATIO CLUSTERS

$\mathcal{R}_{\text{Si}}^{\text{Al}}$  vs  $\mathcal{R}_{\text{Si}}^{\text{Fe}}$  — Clusters in composition space and real space



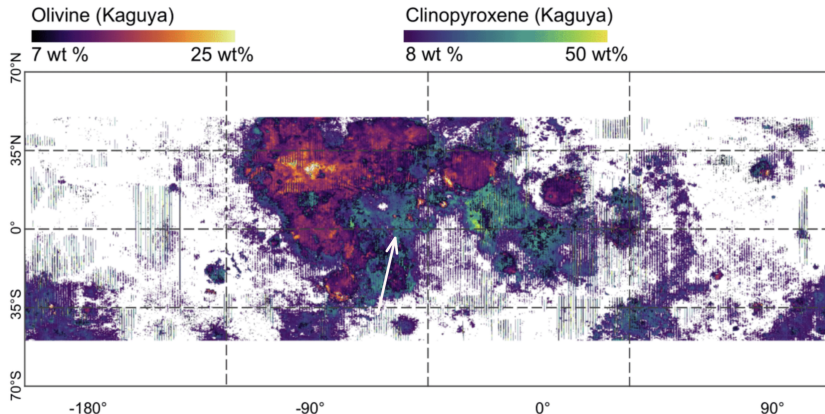
## 2-D RATIO CLUSTERS

$\mathcal{R}_{\text{Si}}^{\text{Al}}$  vs  $\mathcal{R}_{\text{Si}}^{\text{Fe}}$  — Clusters in composition space and real space



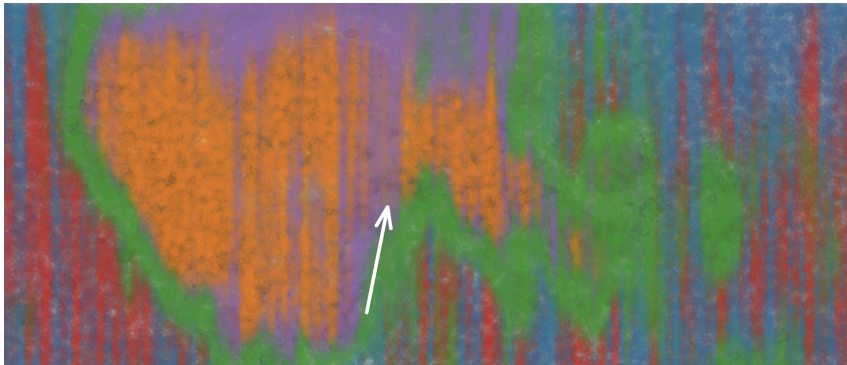
## 2-D RATIO CLUSTERS

$R_{\text{Si}}^{\text{Al}}$  vs  $R_{\text{Si}}^{\text{Fe}}$  — Comparison with mineralogy mappers from Thoresen et al. [17]



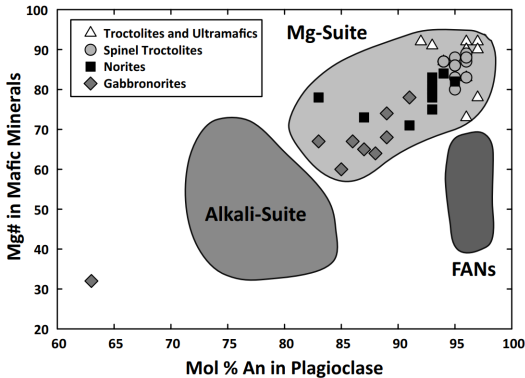
## 2-D RATIO CLUSTERS

$\mathcal{R}_{\text{Si}}^{\text{Al}}$  vs  $\mathcal{R}_{\text{Si}}^{\text{Fe}}$  — Comparison of the central Maria region



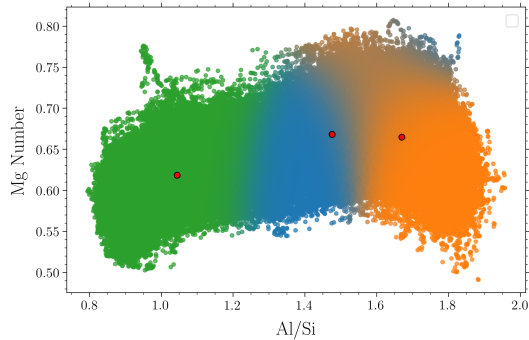
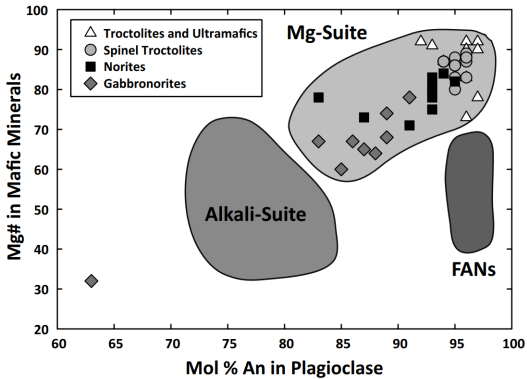
## 2-D RATIO CLUSTERS

Mg# vs  $\mathcal{R}_{\text{Si}}^{\text{Al}}$  – Comparison with Shearer et al. [16]



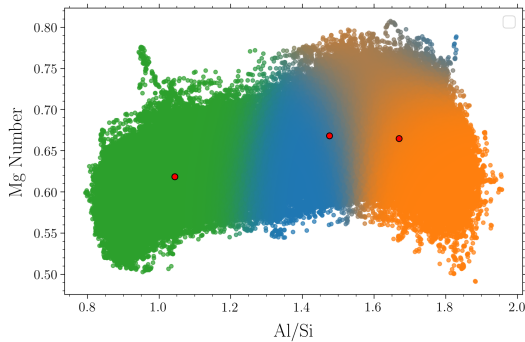
# 2-D RATIO CLUSTERS

Mg# vs  $\mathcal{R}_{\text{Si}}^{\text{Al}}$  — Comparison with Shearer et al. [16]



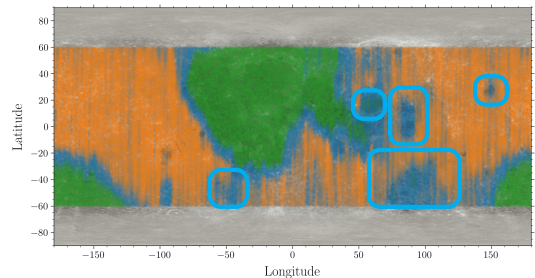
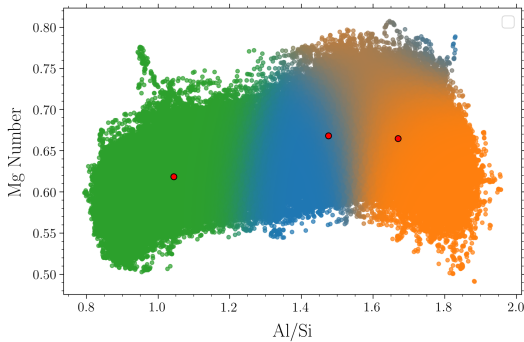
# 2-D RATIO CLUSTERS

Mg# vs  $\mathcal{R}_{\text{Si}}^{\text{Al}}$  — Clusters in composition space and real space



## 2-D RATIO CLUSTERS

Mg# vs  $\mathcal{R}_{\text{Si}}^{\text{Al}}$  — Clusters in composition space and real space



# Thank You

# BIBLIOGRAPHY I



- [1] Astropy Collaboration et al. “Astropy: A community Python package for astronomy”. In: 558, A33 (Oct. 2013), A33. DOI: 10.1051/0004-6361/201322068. arXiv: 1307.6212 [astro-ph.IM].
- [2] Astropy Collaboration et al. “The Astropy Project: Building an Open-science Project and Status of the v2.0 Core Package”. In: 156.3, 123 (Sept. 2018), p. 123. DOI: 10.3847/1538-3881/aabc4f. arXiv: 1801.02634 [astro-ph.IM].
- [3] Astropy Collaboration et al. “The Astropy Project: Sustaining and Growing a Community-oriented Open-source Project and the Latest Major Release (v5.0) of the Core Package”. In: 935.2, 167 (Aug. 2022), p. 167. DOI: 10.3847/1538-4357/ac7c74. arXiv: 2206.14220 [astro-ph.IM].
- [4] Larry Bradley et al. *astropy/photutils: 1.8.0*. Version 1.8.0. May 2023. DOI: 10.5281/zenodo.7946442. URL: <https://doi.org/10.5281/zenodo.7946442>.

## BIBLIOGRAPHY II



- [5] Nicholas Earl et al. *astropy/specutils: v1.18.0*. Version v1.18.0. Oct. 2024. DOI: 10.5281/zenodo.13942238. URL: <https://doi.org/10.5281/zenodo.13942238>.
- [6] Sean Gillies et al. *Rasterio: geospatial raster I/O for Python programmers*. Mapbox, 2013-. URL: <https://github.com/mapbox/rasterio>.
- [7] Sean Gillies et al. *Shapely: manipulation and analysis of geometric objects*. [toblerity.org](https://toblerity.org), 2007-. URL: <https://github.com/Toblerity/Shapely>.
- [8] Gloudemans, A. J. et al. “Re-evaluation of Lunar X-ray observations by Apollo 15 and 16”. In: *AA 649* (2021), A174. DOI: 10.1051/0004-6361/202140321. URL: <https://doi.org/10.1051/0004-6361/202140321>.
- [9] Charles R. Harris et al. “Array programming with NumPy”. In: *Nature 585* (2020), 357–362. DOI: 10.1038/s41586-020-2649-2.

# BIBLIOGRAPHY III



- [10] J. D. Hunter. "Matplotlib: A 2D graphics environment". In: *Computing in Science & Engineering* 9.3 (2007), pp. 90–95. DOI: [10.1109/MCSE.2007.55](https://doi.org/10.1109/MCSE.2007.55).
- [11] James Mason. *INSPIRESat-1/DAXSS (AKA MinXSS-3) Level 1 data available — lasp.colorado.edu*. <https://lasp.colorado.edu/minxss/2022/06/06/inspiresat-1-daxss-aka-minxss-3-level-1-data-available/>. [Accessed 04-12-2024]. 2022.
- [12] Wes McKinney et al. "Data structures for statistical computing in python". In: *Proceedings of the 9th Python in Science Conference*. Vol. 445. Austin, TX. 2010, pp. 51–56.
- [13] Netra S. Pillai et al. "Chandrayaan-2 Large Area Soft X-ray Spectrometer (CLASS): Calibration, In-flight performance and first results". In: *Icarus* 363 (2021), p. 114436. ISSN: 0019-1035. DOI: <https://doi.org/10.1016/j.icarus.2021.114436>. URL: <https://www.sciencedirect.com/science/article/pii/S0019103521001196>.

# BIBLIOGRAPHY IV



- [14] QGIS Development Team. *QGIS Geographic Information System*. QGIS Association. 2024. URL: <https://www.qgis.org>.
- [15] Y. Sharma et al. "The search for fast transients with CZTI". In: *Journal of Astrophysics and Astronomy* 42.2 (2021), p. 73. ISSN: 0973-7758. DOI: 10.1007/s12036-021-09714-6. URL: <https://doi.org/10.1007/s12036-021-09714-6>.
- [16] Charles K. Shearer et al. "Origin Of The Lunar Highlands Mg-Suite: An Integrated Petrology, Geochemistry, Chronology, And Remote Sensing Perspective". In: *American Mineralogist* 100.1 (2015), pp. 294-325. DOI: doi:10.2138/am-2015-4817. URL: <https://doi.org/10.2138/am-2015-4817>.
- [17] Freja Thoresen et al. *Insights into Lunar Mineralogy: An Unsupervised Approach for Clustering of the Moon Mineral Mapper (M3) spectral data*. 2024. arXiv: 2411.03186 [astro-ph.EP]. URL: <https://arxiv.org/abs/2411.03186>.

# BIBLIOGRAPHY V



- [18] Freja Thoresen et al. *Insights into Lunar Mineralogy: An Unsupervised Approach for Clustering of the Moon Mineral Mapper (M3) spectral data*. 2024. arXiv: 2411.03186 [astro-ph.EP]. URL: <https://arxiv.org/abs/2411.03186>.
- [19] Guido Van Rossum and Fred L. Drake. *Python 3 Reference Manual*. Scotts Valley, CA: CreateSpace, 2009. ISBN: 1441412697.
- [20] Pauli Virtanen et al. “SciPy 1.0: Fundamental Algorithms for Scientific Computing in Python”. In: *Nature Methods* 17 (2020), pp. 261-272. DOI: 10.1038/s41592-019-0686-2.
- [21] Chen Yang et al. “Comprehensive mapping of lunar surface chemistry by adding Chang'e-5 samples with deep learning”. In: *Nature Communications* 14.1 (2023), p. 7554. ISSN: 2041-1723. DOI: 10.1038/s41467-023-43358-0. URL: <https://doi.org/10.1038/s41467-023-43358-0>.

# APPENDIX

## Gaussian Thresholds

$$\begin{aligned}\text{Amp}(\mathcal{G}) &\geq N\sigma(\text{Amp}(\mathcal{B})) \\ \mu(\mathcal{G}) - E_T &\in [-0.05, 0.05] \\ \sigma(\mathcal{G}) &\in [0.05, 0.1]\end{aligned}$$

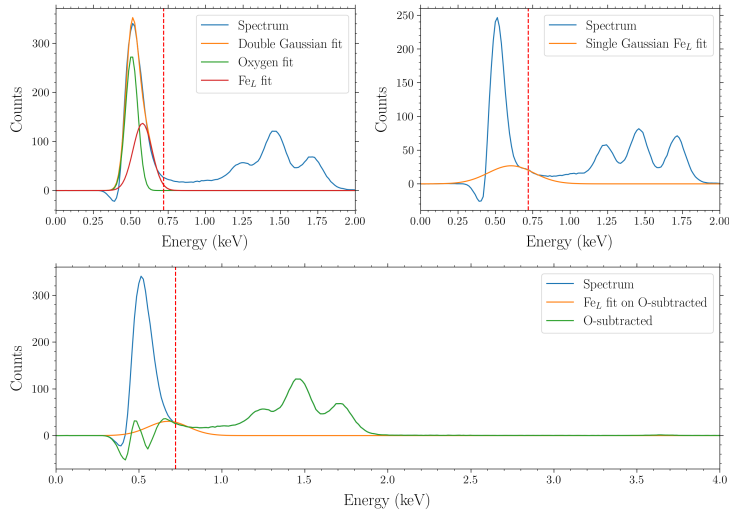
# Fe<sub>L</sub> HIGH SD

---



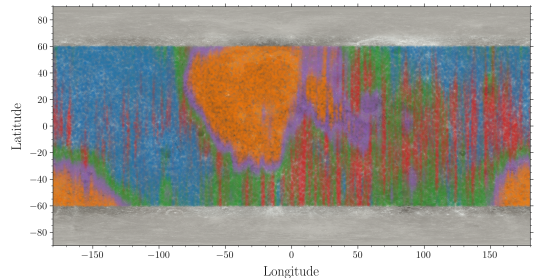
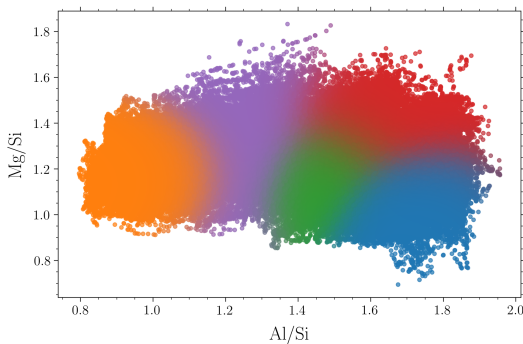
Possibly because of the presence of two close lines, L<sub>α<sub>1</sub></sub> at 0.705 keV and L<sub>β<sub>1</sub></sub> at 0.718 keV

# Fe<sub>L</sub> FITTING



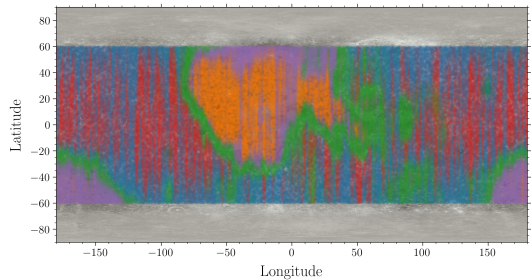
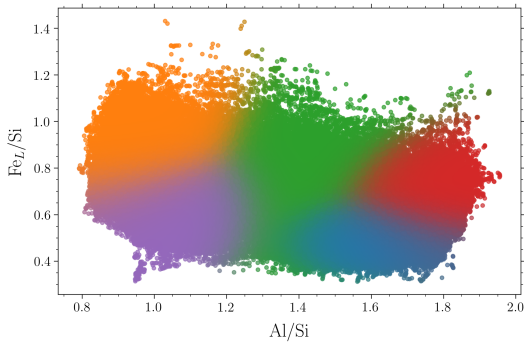
# OTHER 5 GMM FITS

$\mathcal{R}_{\text{Si}}^{\text{Al}}$  vs  $\mathcal{R}_{\text{Si}}^{\text{Mg}}$



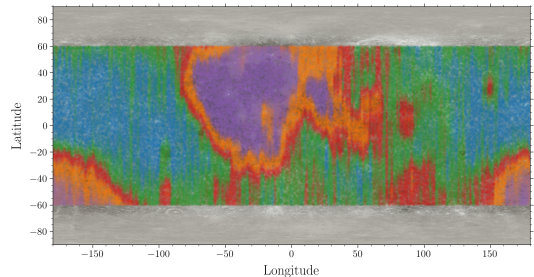
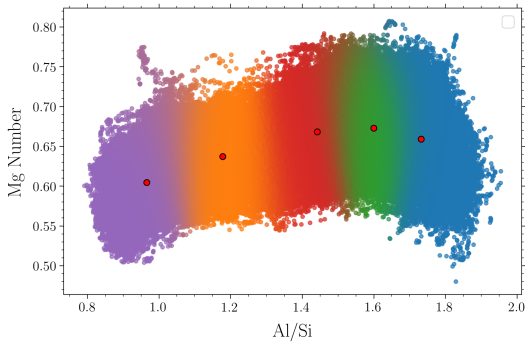
# OTHER 5 GMM FITS

$\mathcal{R}_{\text{Si}}^{\text{Al}}$  vs  $\mathcal{R}_{\text{Si}}^{\text{Fe}}$



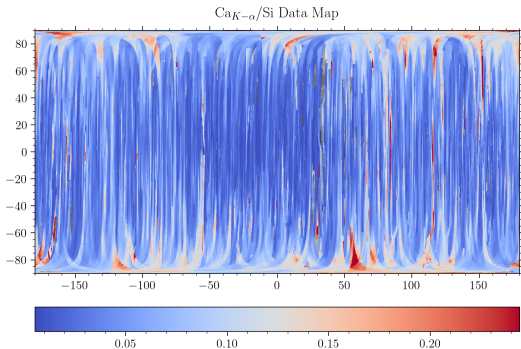
# OTHER 5 GMM FITS

$\mathcal{R}_{\text{Si}}^{\text{Al}}$  vs Mg

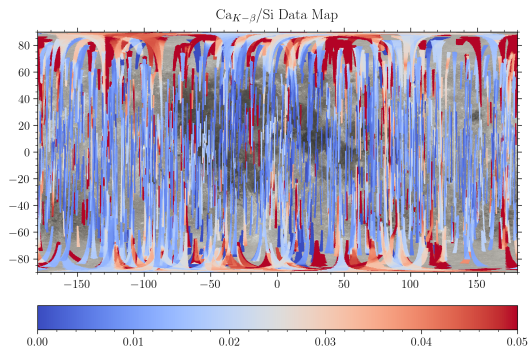


# CALCIUM MAPS

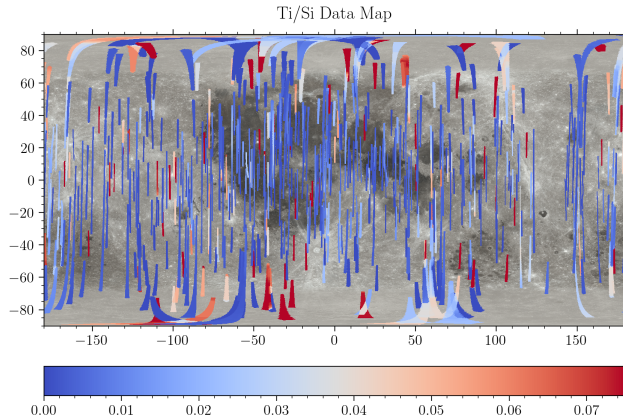
Ca K- $\alpha$  / Si Data Map



Ca K- $\beta$  / Si Data Map

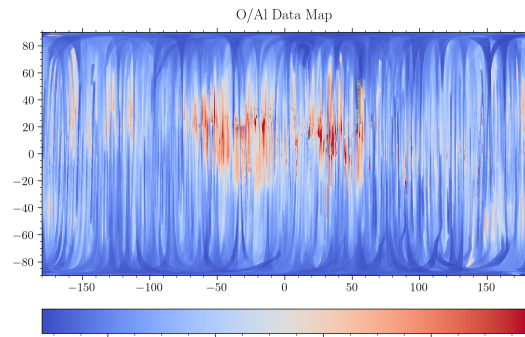
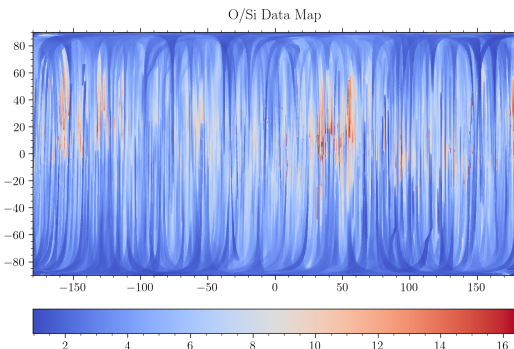


# TITANIUM MAP



# OXYGEN MAPS

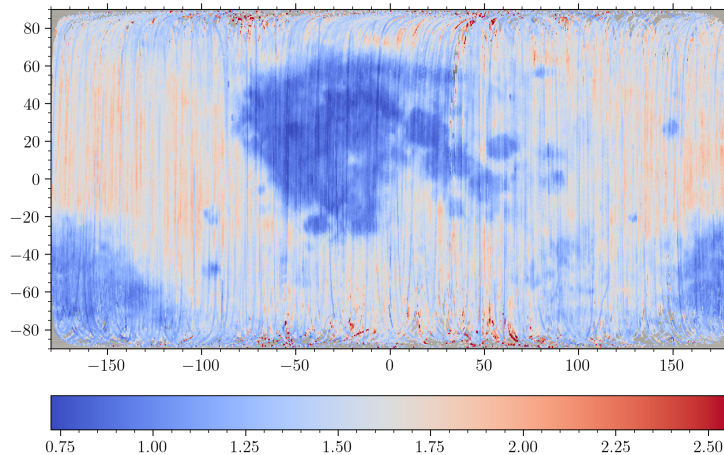
ISRO Problem Statement



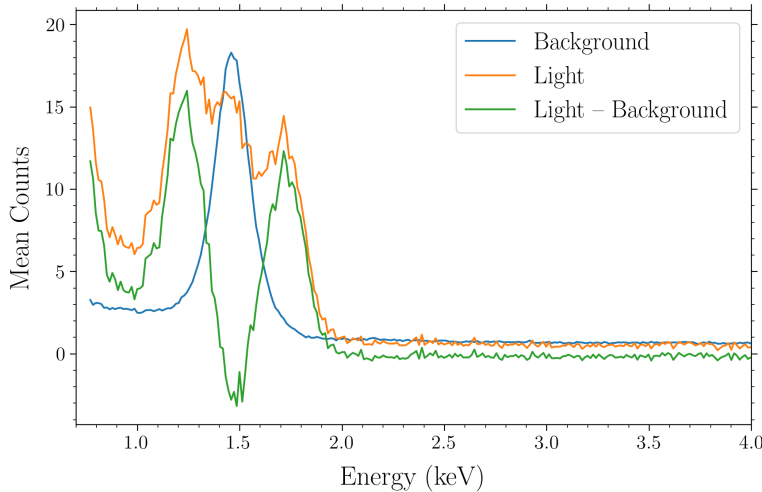
# 48 S TIMEBIN



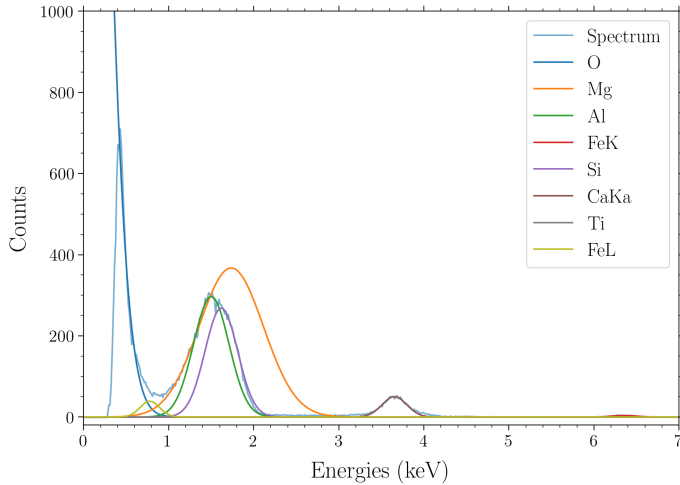
Al/Si Data Map (Timebin = 48 s)



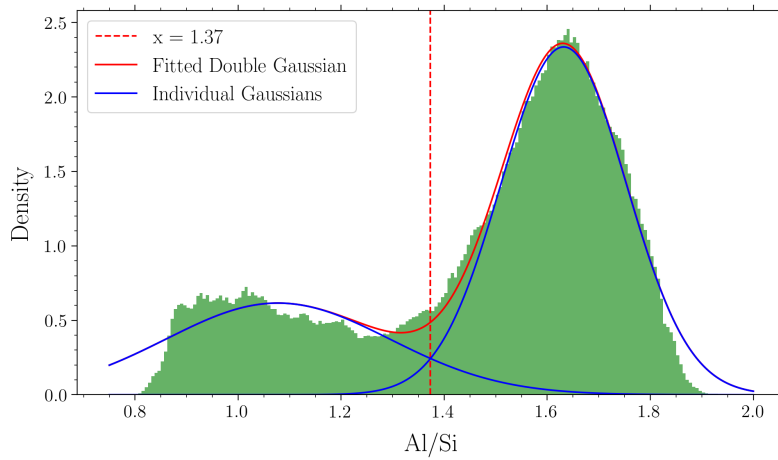
# OVERSUBTRACTED ALUMINUM LINE



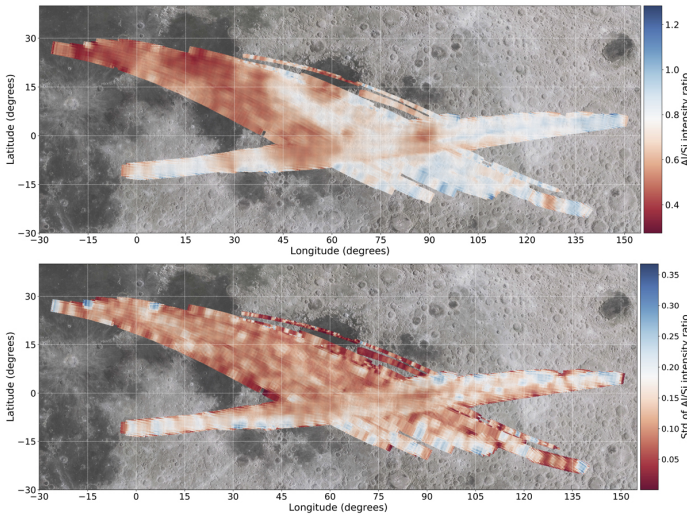
# BAD GAUSSIAN FITS



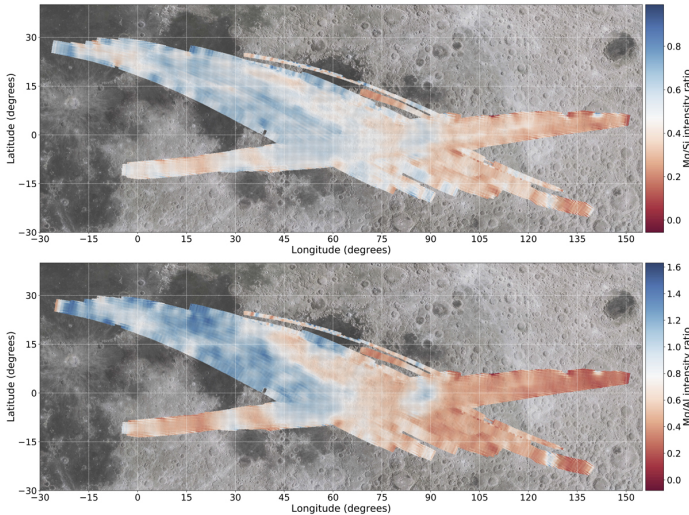
# DOUBLE GAUSSIAN FITTING OF AL RATIO HISTOGRAM

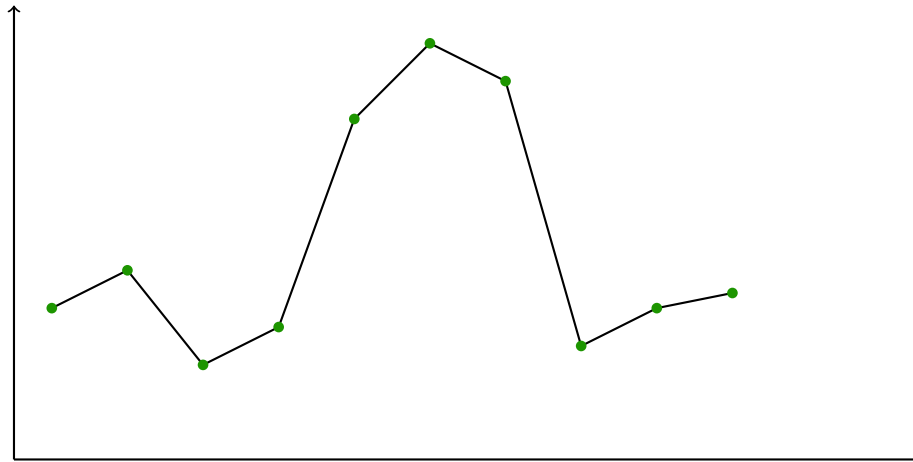


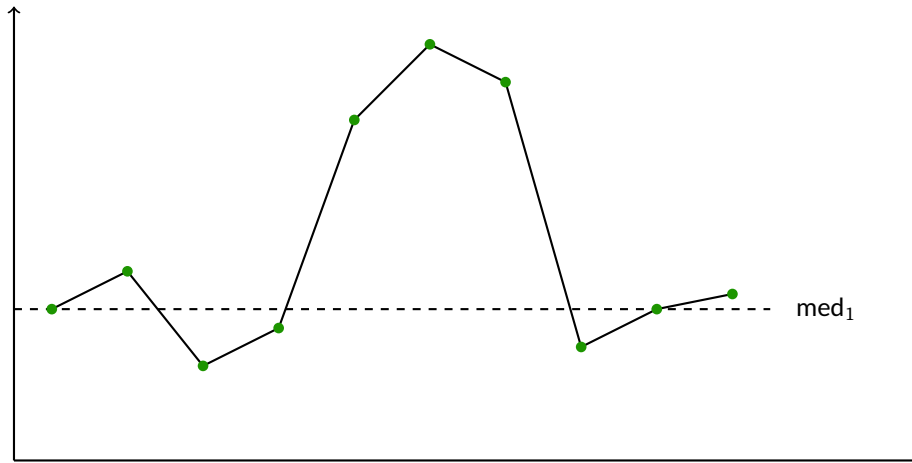
# APOLLO 15/16 AL/SI MAP

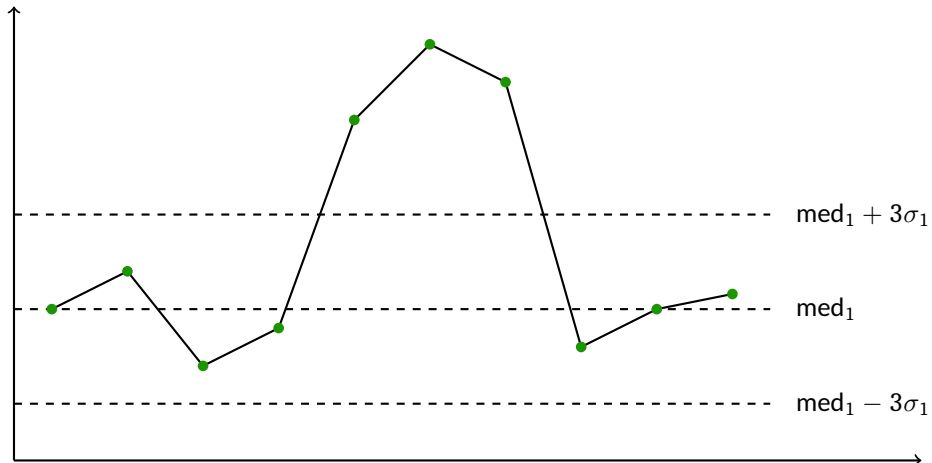


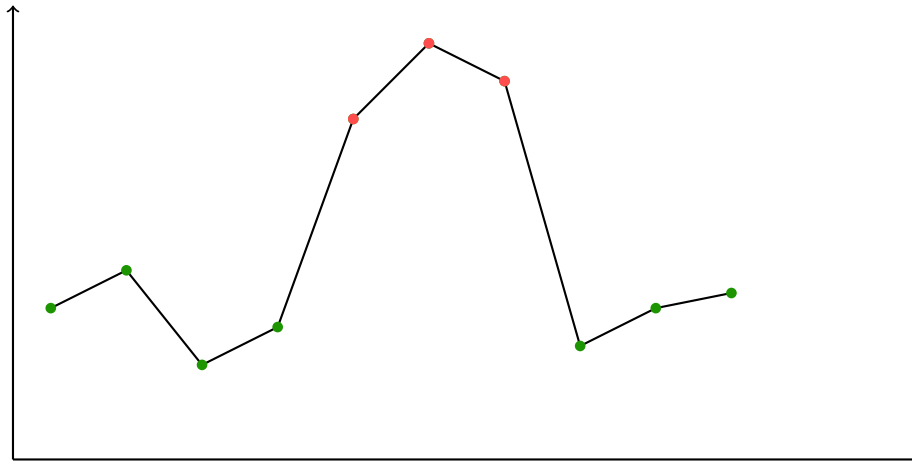
# APOLLO 15/16 MG/SI & MG/AL MAP

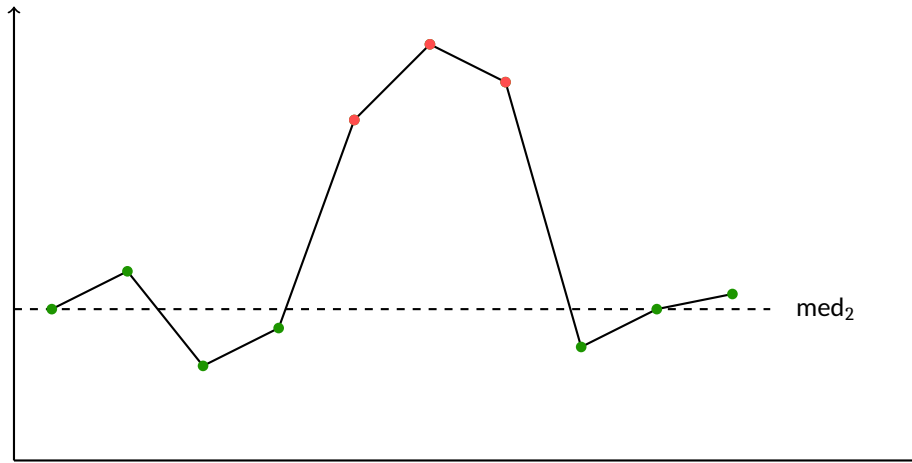


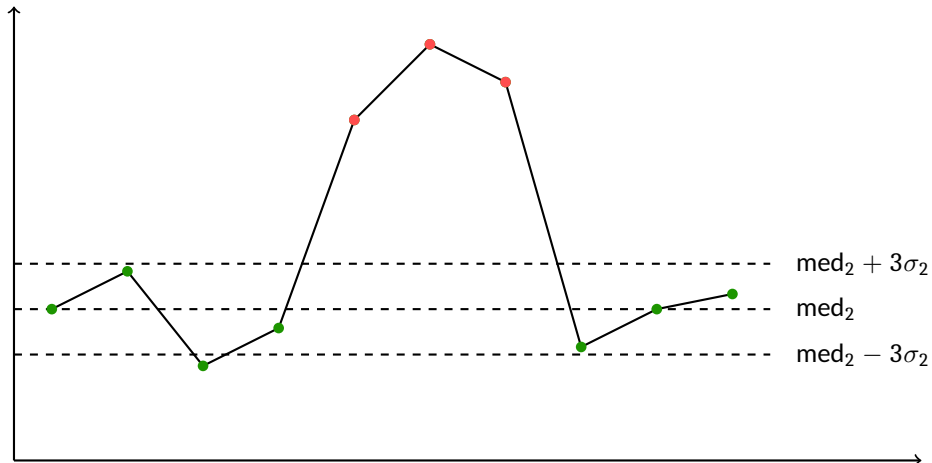


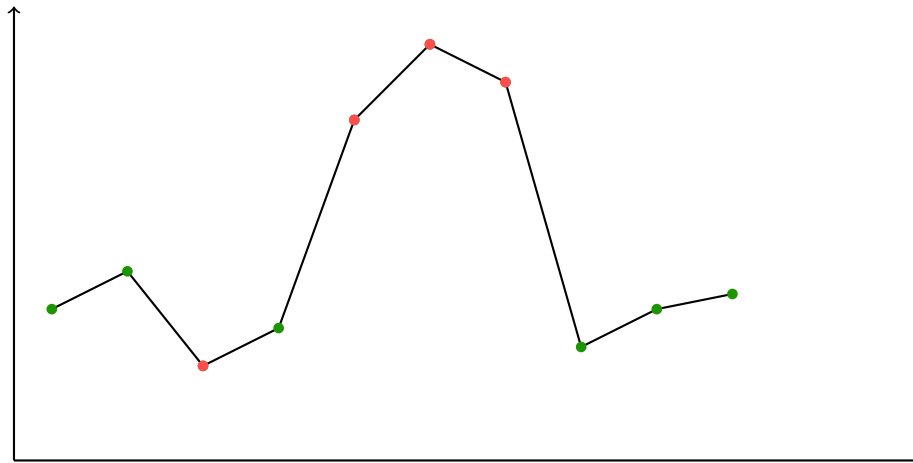


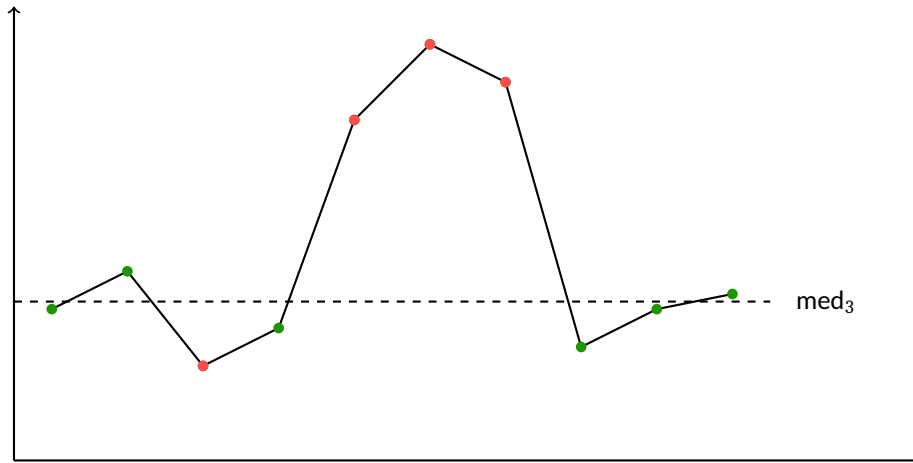


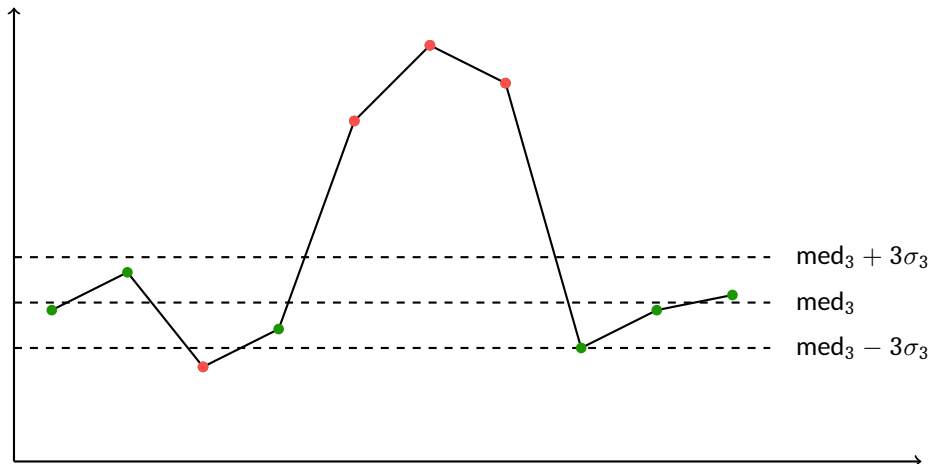


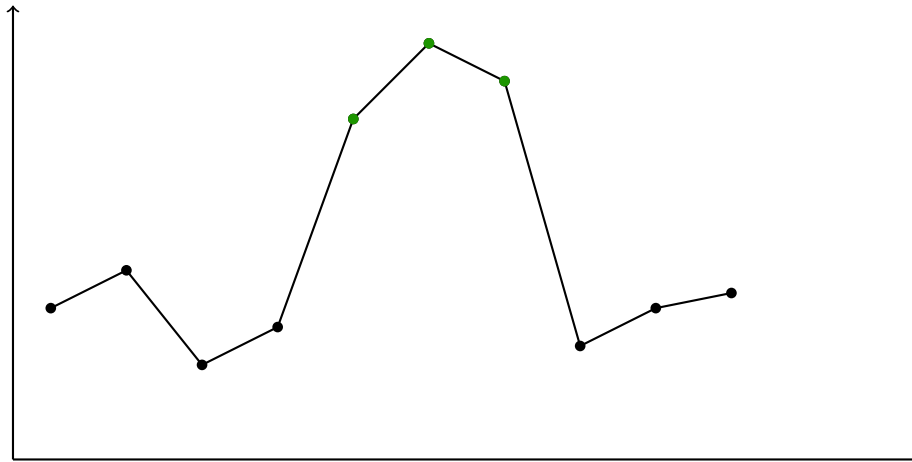


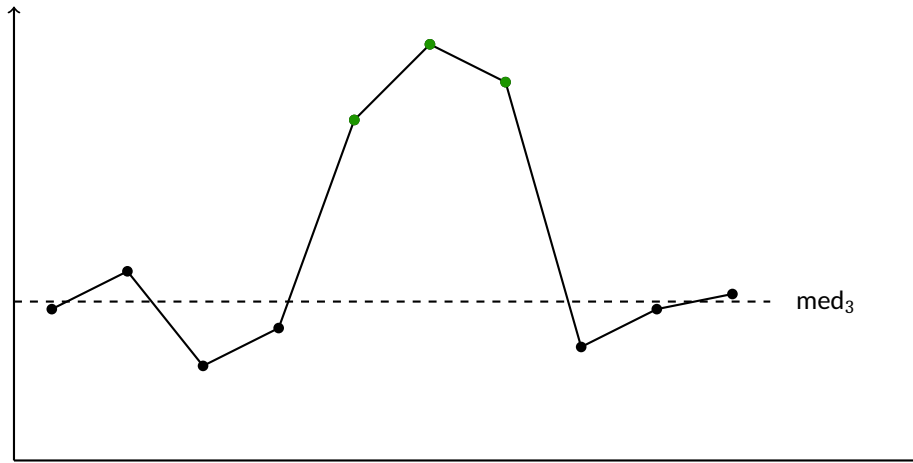


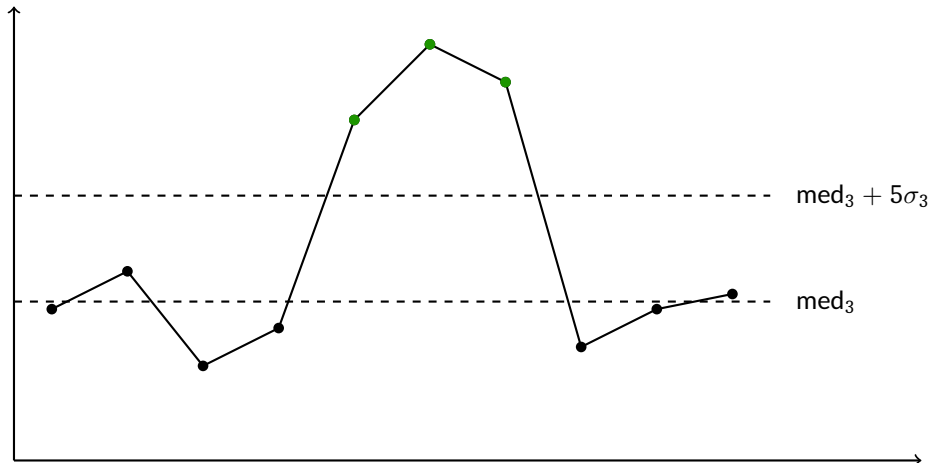








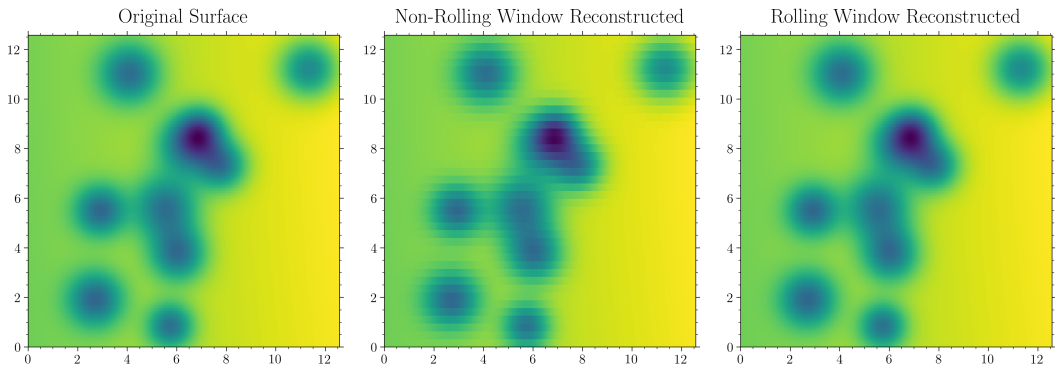




# LIBRARIES USED

- » Python v3.10.15 [19]
- » NumPy [9]
- » SciPy [20]
- » Astropy [1, 2, 3]
- » Pandas [12]
- » Matplotlib [10]
- » Specutils [5]
- » Rasterio[6]
- » Shapely [7]
- » QGIS[14]

# ROLLING WINDOW



# ROLLING WINDOW

Rolling Window

